DIFFERENTIAL INFLUENCE OF LIFE CYCLE ON GROWTH AND TOXIN PRODUCTION OF THREE *PSEUDO-NITZSCHIA* SPECIES (BACILLARIOPHYCEAE)[1]

Aurore SAUVEY
Normandie Univ, UNICAEN, CNRS, BOREA, 14000 Caen, France
Unité Biologie des Organismes et Ecosystèmes Aquatiques (BOREA), Muséum National d'Histoire Naturelle, Sorbonne Université, Université de Caen Normandie, Université des Antilles, CNRS, IRD, 14000 Caen, France

Pascal CLAQUIN
Normandie Univ, UNICAEN, CNRS, BOREA, 14000 Caen, France
Unité Biologie des Organismes et Ecosystèmes Aquatiques (BOREA), Muséum National d'Histoire Naturelle, Sorbonne Université, Université de Caen Normandie, Université des Antilles, CNRS, IRD, 14000 Caen, France

Bertrand LE ROY
Normandie Univ, UNICAEN, CNRS, BOREA, 14000 Caen, France
Unité Biologie des Organismes et Ecosystèmes Aquatiques (BOREA), Muséum National d'Histoire Naturelle, Sorbonne Université, Université de Caen Normandie, Université des Antilles, CNRS, IRD, 14000 Caen, France

Mickael LE GAC
Ifremer, DYNECO PELAGOS, 29280 Plouzané, France

Juliette FAUCHOT[2]
Normandie Univ, UNICAEN, CNRS, BOREA, 14000 Caen, France
Unité Biologie des Organismes et Ecosystèmes Aquatiques (BOREA), Muséum National d'Histoire Naturelle, Sorbonne Université, Université de Caen Normandie, Université des Antilles, CNRS, IRD, 14000 Caen, France
e-mail: juliette.fauchot@unicaen.fr
Phone: (+33)2 31 56 58 37
Fax: (+33)2 31 56 53 46

Condensed running title: Life cycle and *Pseudo-nitzschia* toxin

ABSTRACT

We used a multi-strain approach to study the intra- and interspecific variability of the growth rates of three *Pseudo-nitzschia* species – *P. australis*, *P. fraudulenta,* and *P. pungens* – and of their domoic acid (DA) production. We carried out mating and batch experiments to investigate the respective effects of strain age and cell size, and thus the influence of their life cycle on the physiology of these species. The cell size - life cycle relationship was characteristic of each species. The influence of age and cell size on the intraspecific variability of growth rates suggests that these characteristics should be considered cautiously for the strains used in physiological studies on *Pseudo-nitzschia* species. The results from all three species do not support the hypothesis of a decrease in DA production with time since isolation from natural populations. In *P. australis*, the cellular DA content was rather a function of cell size. More particularly, cells at the gametangia stage of their life cycle contained up to six times more DA than smaller or larger cells incapable of sexual reproduction. These findings reveal a link between *P. australis* life cycle and cell toxicity. This suggest that life cycle dynamics in *Pseudo-nitzschia* natural populations may influence bloom toxicity.

KEY WORDS: domoic acid, cell size, growth, life cycle, *Pseudo-nitzschia* strains

ABBREVIATIONS: DA, domoic acid; cDA, cellular domoic acid; dDA, extracellular dissolved domoic acid.

INTRODUCTION

Diatoms are one of the most common eukaryotic phytoplankton groups in aquatic environments, with approximately 100,000 different species recorded (Not et al. 2012, Mann and Vanormelingen 2013). This ecological success has previously been related to different characteristics of diatoms: the presence of their unique siliceous cell wall, the frustule (Hamm et al. 2003, Armstrong et al. 2009), some metabolic particularities (Allen et al. 2011, Bailleul et al. 2015), important intraspecific diversity (Godhe and Rynearson 2017), and also their unique life cycle (Lewis 1984, 1987). This life cycle is strongly related to variations in cell size, and characterized by two phases: long periods of vegetative multiplication, and short sexual events. During the vegetative phase, cell size decreases over the generations until reaching a minimum non-viable size. This decrease in size is one of the consequences of the presence of the silicified rigid cell wall called a frustule, which is typical of diatoms. While size decreases, vegetative diatom cells are only capable of sexual reproduction within a specific size range corresponding to the gametangia stage. Sexual reproduction then leads production of gametes through meiosis followed by fusion to produce a zygote; then the zygote enlarges to produce a specialized structure called an auxospore allowing for the regeneration of an initial cells of maximum size (Mann 1999, Chepurnov et al. 2004, Kaczmarska et al. 2013). The control of sexual reproduction by cell size affects the frequency, the timing, and the importance of sexual reproduction events (D'Alelio et al. 2010, Hense and Beckmann 2015). These in turn probably affect bloom dynamics in natural populations. The link between cell size and life cycle is thus an important characteristic to be explored in diatoms. Furthermore, as far as cell metabolism is concerned, according to allometric laws small cells are generally considered more competent physiologically than larger cells (*e.g.* thanks to better growth or nutrient acquisition; Edwards et al. 2012, Marañón et al. 2013, Otero et al. 2018), even if some authors reported a decrease in growth rate for smaller cells linked to certain life cycle stages (Chisholm and Costello 1980, Von Dassow et al. 2006). However, the influence of cell size reduction on diatom physiology as related to the life cycle is still poorly documented.

The heterothallic pennate diatoms of the genus *Pseudo-nitzschia* are cosmopolitan. Fifty species of *Pseudo-nitzschia* are currently described, out of which 24 are considered to be toxic, *i.e.* capable of producing domoic acid (DA), a neurotoxin that will accumulate in marine food webs and cause amnesic shellfish poisoning (ASP) events (Lelong et al. 2012 and references herein, Lim et al. 2013, Orive et al. 2013, Fernandes et al. 2014, Teng et al. 2014, 2016, Li et al. 2017, Ajani et al. 2018, Frøsig Gai et al. 2018). According to the literature on different *Pseudo-nitzschia* species, important interspecific differences in DA cellular content exist (*e.g.* Pan et al. 1996a and 1996b,

Fehling et al. 2004, Howard et al. 2007, Lelong et al. 2012, Thorel et al. 2014, Martin-Jézéquel et al. 2015, Radan and Cochlan 2018). However, a few authors studied several strains *per* species and also reported significant intraspecific diversity (*e.g.* Garrison et al. 1992, Villac et al. 1993, Álvarez et al. 2009). Intraspecific diversity in DA production was even higher than interspecific diversity in *P. multiseries*, *P. calliantha,* and *P. fraudulenta* from USA coastal waters (Thessen et al. 2009). In contrast, interspecific differences in DA production were greater than intraspecific variability in three *P. australis*, *P. pungens* and *P. fraudulenta* strains from the French coastal waters (Lema et al. 2017). These authors also pointed out that the time spent in culture since isolation might influence *Pseudo-nitzschia* species physiology, including DA production, as previously reported by Lelong et al. (2012). In addition, previous studies concluded that cell size reduction induced a decrease in DA production in several *Pseudo-nitzschia* species (Bates et al. 1999, Mafra et al. 2009, Amato et al. 2010).

The objective of this study was therefore to investigate the inter- and intraspecific variability of growth and domoic acid production in three *Pseudo-nitzschia* species from the French coastal waters, namely *P. australis*, *P. pungens,* and *P. fraudulenta*. We applied a multi-strain approach to grasp intraspecific variability, by studying at least nine strains *per* species. In addition, we made a special effort to explore the influence of the life cycle on the physiology of each species by studying strains of different cell sizes and the same strains at different sizes during the cell size reduction process. This also allowed us to investigate the influence of strain age on growth and toxin production. Improving knowledge of intraspecific variability in *Pseudo-nitzschia* species is required for an accurate characterization of the physiology of each species, and thus a better understanding of their harmful bloom dynamics.

MATERIALS AND METHODS

Strains

Some *Pseudo-nitzschia* spp. strains were isolated from natural populations: from the west coast of Brittany and in Arcachon Bay (Atlantic coast, France) for *P. australis,* and from the Bay of Seine (English Channel, France) for *P. pungens* and *P. fraudulenta.* Other strains were obtained by isolating initial cells produced during sexual reproduction experiments (Table 1). Single cells or short chains were isolated using a micropipette, washed three times with filter-sterilized (0.2 µm) seawater, and incubated in 4-well culture plates in K/2-medium (Keller et al. 1987) enriched in Si (54 µM) at a temperature of 16°C, an irradiance of 30 µmol photons.m^{-2}.s^{-1}, and a 14:10 L:D light

cycle. When the clonal culture was established, it was maintained in 15 ml ventilated flasks in K/2-medium + Si in the same conditions. Cultures were not axenic, but they were periodically checked for bacterial development by optical microscopy observations, and hardly any bacteria were detected. Most *Pseudo-nitzschia* species were identified from measurements of frustule properties by transmission electron microscopy (TEM) and some by molecular sequencing of the entire internal transcribed spacer region (ITS1-5.8S-ITS2) of the ribosomal RNA (see Lema et al. 2017). For TEM observations, samples were cleaned to remove organic material according to Thorel et al. (2017). To characterize the cell size range of each species, the cell size of each strain was measured every month. The minimum cell size was characterized as the minimum viable size in four *P. australis* strains, six *P. fraudulenta* strains, and six *P. pungens* strains. The strains were observed under a Nikon Eclipse 80i light microscope equipped with a Nikon DS-Ri2 camera, and 20 cells were measured (length and width) using NIS-Elements Imaging Software. Cell apical length (called cell size here) was calculated as the mean ± standard deviation of each batch of 20 cells (Lundholm et al. 2002).

Experiment 1: Mating experiments

The main objective of these experiments was to link *Pseudo-nitzschia* spp. cell size to shifts in life cycle stages, especially by defining the gametangia and the initial cell size ranges. Mating experiments were carried out monthly with *P. australis*, *P. pungens*, and *P. fraudulenta* strains in the course of their cell size reduction process for one year. Strains were considered at the gametangia stage when they were capable of sexual reproduction. These experiments also provided large-size strains from initial cells (F1 strains). Before carrying out the experiments, the cultures (Table 1) were acclimated to the experimental conditions (16°C, 100 µmol photons.m^{-2}.s^{-1} and 14:10 L:D light cycle), and 20 cells from each culture were measured. Mating experiments were performed in 6-well culture plates in 5 ml of K/2-medium + Si, with an initial concentration of 5,000 cells.ml^{-1} for each of the two strains of the compatible mating type. The mating type was assessed by crossing the strains with reference strains of known mating types. The strain that bore the auxospores was defined as “PN-”, and the other one as “PN+” (Kaczmarska et al. 2013). Plates were incubated in growth chambers at 16°C, 100 µmol photons.m^{-2}.s^{-1} and 14:10 L:D light cycle (Economic Delux, Snijders Scientific B. V., UK). The crosses were checked daily for the formation of sexual stages (gametes, zygotes, auxospores, or initial cells) under an inverted light microscope (Leica DMIL LED, Wetzlar, Germany). Initial cells were sampled from the successful crosses, and

20 cells were measured (length and width) under a Nikon Eclipse 80i light microscope equipped with a Nikon DS-Ri2 camera using NIS-Elements Imaging Software.

Experiment 2: Batch experiments

Batch experiments were performed to study two physiological indices, *i.e.* the growth rate and domoic acid production (cellular domoic acid – cDA – and extracellular dissolved DA – dDA – concentrations). The growth rate parameter was estimated during the exponential growth phase, and DA concentrations were measured on the second day of the stationary phase because DA production is higher during this phase before the culture starts declining (Cusack et al. 2002, Fehling et al. 2004, Thessen et al. 2009).

Batch experiments were carried out with *P. australis*, *P. pungens*, and *P. fraudulenta* strains (Table 1). Before each experiment, each strain was acclimated to experimental conditions *i.e.* 16°C, 100 µmol photons.m^{-2}.s^{-1}, and 14:10 L:D light cycle in growth chambers (Economic Delux, Snijders Scientific B.V., UK). The experiments were carried out in 250 ml filter flasks (NEST^{TM}) with 100 ml of K/2 + Si. $Si(OH)_4^-$ and PO_4^{2-} concentrations were modified to obtain phosphate or silicate limitation in the stationary phase because DA production is obtained in *Pseudo-nitzschia* cultures after an exponential growth phase followed by quasi-exhaustion of P or Si which induces growth arrest (Pan et al. 1996a, 1996b, 1998, Fehling et al. 2004, Amato et al. 2010). Nitrogen, phosphorus, and silicon concentrations in the culture medium were as follows: 400 µM $NaNO_3$, 5 µM KH_2PO_4, and 125 µM Na_2SiO_3 for P limitation, and 400 µM $NaNO_3$, 25 µM KH_2PO_4, and 25 µM Na_2SiO_3 for Si limitation. At the beginning of each experiment, an acclimated culture in the exponential growth phase was centrifuged (10 min, 800 g, 16°C) in order to add only cells to the culture medium without affecting nutrient concentrations. The initial cell concentration for all experiments was around $2.5.10^3$ cells.ml^{-1} (± $0.25.10^3$). Samples were collected once a day in the early afternoon to monitor cell concentrations using a Nageotte counting chamber. At the end of the experiment, each flask still contained at least half of the initial volume of culture.

The growth rate was calculated using the following equation:

$$\mu = \frac{ln(X_2) - ln(X_1)}{t_2 - t_1}$$

Where t is time in days, and X_1 and X_2 are cell concentrations (cells.ml^{-1}) at t_1 and t_2, respectively.

On the second day of the stationary phase, samples were taken for DA measurements. A 10 ml aliquot was taken from each flask, centrifuged, and the supernatant was recovered for extracellular dissolved DA (dDA) measurements. A second 10-ml aliquot was sonicated on ice with a sonication probe (Bioblock Scientific Vibracell 72442 ultrasons) for 4 minutes to disrupt cell membranes and release DA from the cells, and filtered on a 0.2-µm filter (33 mm, cellulose acetate membrane). This fraction was used to measure total DA (tDA). The samples were frozen at -20°C prior to analysis. DA quantification was performed using an ASP ELISA kit (Biosense Laboratories, Bergen, Norway) following the manufacturer's instructions. Each sample was analyzed in duplicate for quality control purposes. The absorbance was measured using a microplate spectrophotometer (iMark^{TM} Microplate Absorbance Reader, Bio-Rad Laboratories, Inc) equipped with a 450 nm filter. According to the manufacturer, the calibrated range of the assay is 10 – 300 pg.ml^{-1}.

The cellular domoic acid content (cDA, pg.cell^{-1}) was calculated from tDA and dDA (in pg.ml^{-1}) normalized to the cell concentration (cells.ml^{-1}) as follows:

$$cDA = \frac{tDA - dDA}{cell\ concentration}$$

To characterize interspecific and intraspecific variability in growth and DA production, these batch experiments were performed on multiple strains for each of the three species, *i.e.* nine *P. australis* strains, thirteen *P. pungens* strains, and twelve *P. fraudulenta* strains (Table 1). Potential intraspecific variability may originate from genetic variability among strains, but also from the influence of cell size linked to the life cycle or the influence of the time spent in culture. Therefore, we calculated the age of strains isolated from natural populations as the time spent in culture between the date of isolation and the date of each experiment. It is worth noting that we did not take into account F1 strains when we studied the effect of strain age because they were not isolated from natural population. Some strains (four *P. australis*, three *P. pungens*, and four *P. fraudulenta* strains) were also studied at different cell sizes in the course of the size reduction process to estimate the influence of cell size or time in culture (Table 1). Furthermore, we also performed batch experiments on F1 strains and their parent strains to compare their growth rate and DA production and test whether these were inherited characters or influenced by changes in cell size.

Statistics

After testing the normality and homoscedasticity of the data, ANOVA was used to test differences in initial size, growth rate, cDA and dDA concentrations among the three species using the "car" package in R version 3.5.1. Linear regressions were used to study the effect of cell size or age on the growth rates of *P. australis*, *P. pungens*, and *P. fraudulenta* strains, and cDA or dDA in *P. pungens* and *P. fraudulenta* cells larger or smaller than 60 µm, using the "lm" package in R. Multiple linear regression analyses were performed to study the combined effect of cell size and age on growth rate, using the "lm" package in R. Statistical significance was set at $\alpha = 0.05$ in all tests.

RESULTS

Life cycle characteristics

We characterized the minimum and maximum (initial cells) cell size for each species, along with the size range within which the cells were capable of sexual reproduction – the gametangia size range – to study the influence of the life cycle on *Pseudo-nitzschia* physiology.

The sizes of the initial cells issued from the mating experiments significantly differed among the three species ($P < 0.001$). The initial cell sizes ranged from 134 µm to 167 µm (144 µm on average) for *P. australis*, from 149 µm to 183 µm (162 µm on average) for *P. pungens*, and from 100 µm to 128 µm (113 µm on average) for *P. fraudulenta* (Fig. 1). Globally speaking, the multiple crosses showed that initial cell size was not dependent on parental cell size whatever the species (Fig. 1). The minimum cell size for a species was estimated as the minimum cell size for which cells grew in culture. This mean minimum cell size was 29.5 µm ± 1.7 for *P. australis*, 32.6 µm ± 1.4 for *P. pungens*, and 22.3 µm ± 0.8 for *P. fraudulenta* (Fig. 2). These values corresponded to 17.6 % ± 1.0, 17.8 % ± 0.8, and 17.5 % ± 0.6 of the maximum initial cell size, respectively. Microscopic observations revealed abnormal valve shapes in small-sized cells (Supplementary Fig. 1).

Gametangia sizes ranged from 55 to 85 µm, 43 to 75 µm, and 29 to 90 µm in *P. australis*, *P. pungens*, and *P. fraudulenta*, respectively. These sizes corresponded to 33 - 51 %, 23 - 41 %, and 27 – 70 % of the maximum initial cell sizes, respectively (Fig. 2). These results mean that *P. fraudulenta* cells were at the gametangia stage for 57.5 % of their life cycle, *P. australis* for only 21.6 %, and *P. pungens* 21.3 %, even if these evaluations may have been influenced by variation in division rate with cell size (D'Alelio et al. 2009). These size ranges corresponded to gametangia

capable of producing new initial cells through sexual reproduction. However, the mating experiments revealed that slightly smaller or larger cells were also able to produce gametes that fused to form zygotes; yet, in these parental cell sizes, the resulting auxospores did not fully develop and therefore did not produce initial cells (Fig. 2).

Growth rate: influence of strain age and cell size

The growth rate of *P. australis*, *P. pungens* and *P. fraudulenta* spanned from 0.31 to 0.82 day^{-1}, 0.15 to 0.75 day^{-1} and 0.19 to 0.68 day^{-1}, respectively (Fig. 3B). These results show great intraspecific variability in growth rate in *Pseudo-nitzschia* spp., while no significant difference among the three species emerged. The high diversity of the strains in terms of cell size and age allowed us to explore the relative influence of these two parameters on the growth rate. Even if globally older strains tended to be characterized by smaller cells, there was no simple and direct relationship between the cell size and the age when considering all strains used for one species. Since all strains were not isolated at the same cell size, some strains of the same age exhibited different cell sizes (Supplementary Fig. 2).

In *P. australis*, *P. pungens* and, *P. fraudulenta*, the growth rate decreased significantly with age ($P < 0.001$, Fig. 3A). However, in *P. pungens* and *P. fraudulenta*, we did not study strains of all ages, but rather two groups corresponding to two sampling periods (2011-2012 and 2016, Table 1). Therefore, some strains were more than 40 months old, and others were less than 10 months old. For these two species, although globally growth rate decreased with age, it is worth nothing that no tendency of growth rate evolution as a function of age emerged in either of these two groups taken separately (Fig. 3A).

Globally, for the three species, growth rates were always lower for cell size below 60 µm (Fig. 3B). However, beyond this general tendency, the relationship between cell size and growth rates were species specific. There was no relationship between cell size and growth rate in *P. fraudulenta*, except the difference below and above this threshold of 60 µm. In *P. pungens*, the growth rate decreased linearly with cell sizes above 60 µm, but below this size there was no significant tendency of growth evolution with cell size except that growth rates were the lowest. Finally, in *P. australis*, the growth rate significantly decreased with cell size ($P < 0.001$ above and below 60 µm). However, the decrease was more pronounced when cell sizes were below 60 µm (Fig. 3B).

In each strain cell size decreased with age, as in all diatom cultures, so we used multiple linear regression analyses to discriminate the effect of age from the effect of cell size on the measured growth rates (equations 1A, 1B, 2, and 3).

(1A) *P. australis*, size < 60 µm: $\mu = -0.5113 + 0.0225*Size$ ($P < 0.001$)
(1B) *P. australis*, size > 60 µm: $\mu = 0.3847 + 0.0028*Size$ ($P < 0.001$)
(2) *P. pungens*: $\mu = 0.4563 - 0.0051*Age + 0.0014*Size$ ($P < 0.001$)
(3) *P. fraudulenta*: $\mu = 0.6093 - 0.00481*Age$ ($P < 0.001$)

Even if *P. australis*, growth rate decreased with age and cell size taken separately, the results of this statistical approach show that *P. australis* growth rate could be predicted from cell size alone. *P. australis* strains of different ages exhibited similar growth rates (*e.g.* around 0.60 day^{-1} for 9-month-old or 21-month-old strains), while strains of the same age grew at different rates (*e.g.* 0.60 or 0.30 day^{-1} for 20 month-old strains, Fig. 3A). In contrast, the largest *P. australis* strains (> 60 µm) had the highest growth rates (> 0.60 day^{-1}), and the strains whose cell size was below 45 µm (< 0.45 day^{-1}, Fig. 3B) had the lowest. In *P. pungens*, the growth rate was a function of both cell size and age. The growth rate decreased from around 0.60 to 0.15-0.38 day^{-1} between young (less than 10 months old) and older *P. pungens* strains (more than 40 months old). But these changes in growth rate in *P. pungens* were also linked to changes in cell size: the strains whose cell size was above 60 µm exhibited the highest growth rates, while smaller strains grew slower (Fig. 3B). In contrast, the growth rate of *P. fraudulenta* was only a function of the strain age. For example, the growth rate was between 0.52 and 0.59 day^{-1} for strains less than 10 months old, but between 0.19 and 0.44 day^{-1} for more than 50-month-old *P. fraudulenta* (Fig. 3A).

The life cycle influences toxicity

All the strains of all three species produced domoic acid under our experimental conditions. Whatever the species, there was no significant difference in domoic acid cellular content (cDA) between phosphate limitation and silicate limitation (Supplementary Fig. 3). Even if, for each strain considered individually, cDA could be higher under Si or P limitation (data not shown), there was no global tendency for one limitation to promote higher DA production. In contrast, we measured significant differences among species, with *P. pungens* maximum cDA one order of magnitude

above *P. fraudulenta* maximum cDA, and *P. australis* maximum cDA also one order of magnitude above *P. pungens* maximum cDA ($P < 0.001$, Supplementary Fig. 3).

Figures 4 and 5 show cDA and dDA for the three species, respectively. In *P. australis*, *P. pungens*, and *P. fraudulenta*, cDA was between 12 and 645 fg.cell^{-1}, 0.2 and 50 fg.cell^{-1}, and 0.03 and 5.6 fg.cell^{-1}, respectively (Fig. 4A and 4B). In these three species, dDA was between 0.022 and 8 ng.ml^{-1}, 0.04 and 0.395 ng.ml^{-1}, and 0.03 and 0.215 ng.ml^{-1}, respectively (data not shown). When considering the biomass in the cultures, dDA concentrations corresponded to 1-5,970 fg.cell^{-1} for *P. australis*, 4-90 fg.cell^{-1} for *P. pungens*, and 0.05-10 fg.cell^{-1} for *P. fraudulenta* (Fig. 5A and 5B). The measured dDA concentrations significantly differed among the three species ($P < 0.001$). *P. australis* produced the highest amounts of dDA, followed by *P. pungens*, and then *P. fraudulenta* (Fig. 5A and 5B).

cDA and dDA concentrations were not significantly influenced by strain age in *P. pungens* and *P. fraudulenta*, even if we measured a few higher cDA concentrations in some of the young strains and if no data is available for age between 6 and 40 months (Supplementary Fig. 4B, Fig 5A, and 5B). In *P. australis*, cDA concentrations increased when the strains were between 5 and 12 months old (Supplementary Fig. 4A). However, this increase in cDA seemed to be rather related to *P. australis* cell size (Fig. 4A). The cell size did not affect cDA concentrations in *P. fraudulenta* (Fig. 4B), while dDA concentrations in this species were significantly higher (although very low) in some strains with cell sizes above 75 µm ($P < 0.05$, Fig. 5B). Measured dDA concentrations in *P. pungens* were not related to cell size (Fig. 5B). There was no clear relationship between cDA concentrations and *P. pungens* cell size (Fig. 4B). However, we recorded the highest cDA concentrations for this species (> 20 fg.cell^{-1}) only in the large strains (> 70 µm), although some large-size strains also exhibited very low cDA concentrations. Furthermore, no clear relationship appeared between the cDA or dDA concentrations in F1 strains as compared to their parental strains whatever the species (data not shown).

There was a strong relationship between DA and cell size in *P. australis*. Measured cDA concentrations varied with cell size following a Gaussian model ($P < 0.001$, Fig. 4A):

(4) $$cDA = 524 * e^{(-0{,}5 * (\frac{Size - 71}{18})^2)}$$

cDA concentrations increased from 130 to 425 fg.cell^{-1} as cell size decreased from ~130 to 80 µm. Maximum cDA concentrations were between 600 and 645 fg.cell^{-1} for cell sizes between 62.7 and

69.1 µm. The Gaussian model gave a maximum cDA concentration for 71-µm cells. Below 60 µm, cDA concentrations decreased down to 10 fg.cell^{-1} (Fig. 4A). These results were confirmed by monitoring four *P. australis* strains whose cDA concentrations followed the Gaussian model over time while the cells were decreasing in size (Fig. 6). These results show that large (100 - 130 µm) and small (40 - 30 µm) *P. australis* strains could present cDA concentrations comparable to those of *P. pungens* strains (Fig. 4). Therefore, the difference in cDA between *P. australis* and the other two species was greater in the size range around 50-100 µm. Furthermore, in *P. australis*, measured dDA concentrations also increased in 70 -100 µm strains (Fig. 5A). It is interesting to note that the cell size range for which cDA concentrations were higher in *P. australis* coincided with the size range characteristic of gametangial cells capable of sexual reproduction for this species (55-85 µm, Fig. 2). dDA concentrations were also higher in the upper part of the gametangial cell size range (70-85 µm).

DISCUSSION

Using a multi-strain approach for three *Pseudo-nitzschia* species, we studied the intra- and interspecific variability of growth rates and toxicity. This approach made it possible to disentangle the respective effects of strain age and cell size. Furthermore, taking into account cell size offered a unique perspective on the influence of the life cycle on the physiology of *Pseudo-nitzschia* species.

Cellular and dissolved domoic acid production in P. australis, P. pungens, and P. fraudulenta

Pseudo-nitzschia species are not all systematically toxic, and even among toxic species some strains may not be able to produce DA (Lelong et al. 2012). Previous studies on strains of different geographic origins reported great variability in cDA concentrations in *P. pungens* and *P. fraudulenta*. Although *P. fraudulenta* has sometimes been reported to be a non-producer of DA (Hasle 2002, Thessen et al. 2009, Quijano-Scheggia et al. 2010), our *P. fraudulenta* strains exhibited cDA concentrations between 0.03 and 5.6 fg.cell^{-1}. These concentrations are similar to those reported in the review by Trainer et al. (2012, up to 30 fg.cell^{-1}) and in Lema et al. (2017, up to 55 fg.cell^{-1}), though in the lower range of concentrations. For *P.* pungens, in contrast with studies reporting non-toxigenic strains (Villac et al. 1993, Bates et al. 1998 and references therein), each of our strains produced DA, even if the measured cDA concentrations (0.2 - 50 fg.cell^{-1}) were also in the lower range compared with previous studies (Bates et al. 1998, Baugh et al. 2006, Calu et al. 2009, Rhodes et al. 2013, Lema et al. 2017). *P. pungens* and *P. fraudulenta* also consistently

produced dissolved domoic acid. To our knowledge, this is the first report of dDA production by *P. fraudulenta*, in contrast with Baugh et al. (2006) and Lema et al. (2017) who did not detect dDA production by this species. As for cDA, our results confirm variability in dDA production among *P. pungens* strains, in agreement with previous studies. Lema et al. (2017) did not detect any dDA in their *P. pungens* cultures, while Baugh et al. (2006) measured dDA levels similar to the lowest concentrations measured in the present study (at similar cell concentrations).

P. australis produced the highest cDA concentrations (between 12 and 645 $fg.cell^{-1}$), in the same range as those already measured in strains isolated on French coasts (maximum between 30 and 700 $fg.cell^{-1}$, Thorel et al. 2014, Martin-Jézéquel et al. 2015, Lema et al. 2017), but much lower than in strains isolated in Ireland (up to 26,000 $fg.cell^{-1}$, Cusack et al. 2002) and in the East Pacific coastal waters (up to 1,740 $fg.cell^{-1}$ in Chile, Álvarez et al. 2009; up to 1,870 $fg.cell^{-1}$ in Baja California, Santiago-Morales and García-Mendoza 2011; and up to 37,000 $fg.cell^{-1}$ in California, Garrison et al. 1992). These differences in toxicity may point out the existence of different *P. australis* ecotypes with contrasting capacities of DA production, as previously shown for other *Pseudo-nitzschia* species by Thessen et al. (2009). In the present study, *P. australis* also produced the highest dDA concentrations, in accordance with previous reports by Maldonado et al. (2002, up to 7.6 $ng.ml^{-1}$), Martin-Jézéquel et al. (2015, up to 20.1 $ng.ml^{-1}$), and Lema et al. (2017, 430 $fg.cell^{-1}$).

These results confirm the high interspecific variability in DA production already highlighted by Lelong et al. (2012). More particularly, the gradation in toxicity between *P. fraudulenta*, *P. pungens,* and *P. australis* already observed by Lema et al. (2017) on strains from the same area confirms the hypotheses from an *in situ* study in the English Channel relating bloom toxicity to *Pseudo-nitzschia* species diversity (Thorel et al. 2017). However, our results show that the most toxic *P. pungens* strains are as toxic as some *P. australis* strains. Therefore *P. pungens* also has to be considered when dealing with DA toxic events observed in French coastal waters, particularly in the English Channel where *P. australis* is mainly pointed out (Klein et al. 2010, Thorel et al. 2017).

Only few studies present dDA measurements during blooms (*e.g.* Bargu et al. 2008), while impacts on marine organisms have already been documented (Liu et al. 2007). All our strains produced dDA at significant concentrations, even if the extrapolation of dDA concentrations obtained in culture to *in situ* bloom situations is uncertain. Increased knowledge regarding this parameter is required to grasp its impact on marine ecosystems.

Life cycle characteristics in relation to cell size and consequences on sexual reproduction in natural populations

We characterized the link between cell size and life cycle stages in *P. australis*, *P. pungens*, and *P. fraudulenta* by determining initial cell size, the vegetative cell size range, and the gametangia size range. As reported in the literature (Chepurnov et al. 2004, Kaczmarska et al. 2013), these cardinal points of the diatom life cycle were clearly species-specific. The initial cell sizes were between 134 µm and 167 µm for *P. australis*, 149 µm and 183 µm for *P. pungens*, and 100 µm and 128 µm for *P. fraudulenta*. To our knowledge, this is the first report of initial cell size for *P. fraudulenta*. However, the initial cell size range can be even larger in this species: Cusack et al. (2004) reported vegetative cells greater than 128 µm. *P. pungens* initial cell sizes are in agreement with those found by Chepurnov et al. (2005). Moreover, in *P. australis* and *P. pungens*, these sizes are similar to the initial cell sizes measured during a sexual reproduction event observed *in situ* during a bloom in Washington coastal waters (Holtermann et al. 2010). The relationship between the size of parental cells and the initial cell size has been studied in different pennate and centric diatoms. Some authors report a linear relationship both in centric (Jewson 1992) and pennate diatoms (Davidovich 1994, Edlund and Bixby 2001, Davidovich et al. 2010). However, Armbrust and Chisholm (1992), Davidovich (1994) and Fuchs et al. (2013) observed no relationship between parental size and initial cell sizes in *Thalassiosira weissflogii*, *Fragilariopsis kerguelensis*, and *Synedra tabulata*, respectively. In the present study, the initial cell size was also independent of the parent cell size in all three *Pseudo-nitzschia* species within the studied size range.

Minimum sizes were 28 µm, 31 µm, and 22 µm in *P. australis*, *P. pungens*, and *P. fraudulenta*, respectively. These values are close to those obtained for *P. pungens* (25-30 µm) by Chepurnov et al. (2005) or for *P. arenysensis* (~18 µm) in a laboratory study (Amato et al. 2005) and with a model of size reduction (Schwarz et al. 2009). Interestingly, the minimum cell size corresponded to 17.6 % ± 0.8 of the maximum initial size for the three species. It could be interesting to explore if this threshold of 17 % is valid for other diatom species. These very small cells are rarely observed *in situ* and may not be representative of natural populations for physiological studies.

The gametangia size ranges observed in this study are in accordance with the size range favorable to sexual reproduction usually admitted for diatoms (~30-75 %, Mann et al. 2003, Chepurnov et al. 2004, Von Dassow et al. 2006, Davidovich et al. 2012, Fuchs et al. 2013, Vanormelingen et al. 2013). The three species presented closed gametangia size ranges, since the

475 cells lost their ability to reproduce sexually before reaching the minimum viable cell size
476 (Chepurnov et al. 2004). These gametangia size ranges fall within previous ranges measured for
477 *Pseudo-nitzschia* species: 20-90 % for *P. arenysensis* (Amato et al. 2005), 23-70 % for *P.*
478 *multiseries* (Hiltz et al. 2000), 39-71 % for *P. multistriata* (D'Alelio et al. 2009), although *P.*
479 *australis* and *P. pungens* presented narrower gametangia size ranges. For example, Chepurnov et al.
480 (2005) found that their *P. pungens* strains could mate in a wider size range (20-60 % of initial cell
481 size, according to their data), even if their strains belonged to the same clade as ours (clade I, Lim et
482 al. 2014). When gametangia size ranges are narrower, it can be hypothesized that a smaller portion
483 of the population is capable of sexual reproduction in natural populations. This may affect
484 encounter rates during blooms, and in turn reproductive success. However, the fact that only a small
485 portion of the population can sexually reproduce may also be an ecological advantage regarding
486 competition with the rest of the phytoplankton community because most of the *Pseudo-nitzschia*
487 population would carry on with vegetative multiplication during a sexual reproduction event (Lewis
488 1984). Furthermore, in *P. australis* and *P. pungens*, the narrower gametangia size range is linked to
489 the fact that vegetative cells need to decrease more in size to reach the gametangia stage. These life
490 cycle characteristics probably affect the frequency and the timing of sexual reproduction events in
491 natural populations (Lewis 1984). The difference in gametangia size range observed in the three
492 species therefore suggests that their natural populations could present different sexual reproduction
493 dynamics. This in turn could influence the general population and bloom dynamics (Jewson 1992,
494 Edlund and Stoermer 1997, D'Alelio et al. 2010).
495
496 This study highlights an intermediate stage of the *Pseudo-nitzschia* life cycle. Our
497 experiments revealed a size range wider than that of gametangia, within which cells were capable of
498 gametogenesis and fertilization but could not produce initial cells. This second size range observed
499 for the first time in this study suggests that the metabolic changes linked to the transition from
500 vegetative cells to gametangia occur progressively during the decrease in cell size allowing cells to
501 acquire the ability to reproduce sexually. When entering the larger size range, cells seem to acquire
502 the physiological abilities required for pairing, gametogenesis, and fertilization. This may include
503 production of pheromones for the recognition of complementary sexual types (Sato et al. 2011,
504 Gillard et al. 2013, Frenkel et al. 2014), and mobility abilities for active pairing. In addition, in the
505 larger size range, cells must be physiologically ready for meiosis which leads to gametogenesis
506 (diatom are diplonts). Then, as the cells enter the narrower size range, they probably acquire
507 supplementary physiological abilities that enable them to ensure complete auxosporulation. This
508 process represents a high metabolic cost for the cells: they probably stop most syntheses during at

least the first steps of sexual reproduction that lasts two to four days on average in *Pseudo-nitzschia* species (Davidovich and Bates 1998; Sauvey unpublished data). The zygote also needs lots of storage to restore a new large initial cell (Chepurnov et al. 2005). Therefore, in contrast to cells in the larger size range, gametangial cells in the narrower range may present a more efficient metabolism with higher storage capabilities – especially for silicium – to be able to synthesize the frustule of the new initial cell. These results stress the fact that gametangial cells probably present particular metabolic characteristics as compared to vegetative cells.

Differential influence of life cycle stages and strain age on growth and DA production in Pseudo-nitzschia species

The time spent in culture seemed to influence *P. fraudulenta* and *P. pungens* growth since growth rates decreased with increasing strain age. However, the strains had been isolated during two distant sampling periods, so it is difficult to tell whether this difference was a consequence of cell adaptation to natural environmental conditions (*i.e.* the difference reflected the period when the population from which the strains were isolated) or a physiological change during the culturing period (*i.e.* the difference reflected strain age) (Lakeman et al. 2009). Further studies with strains of complementary ages are needed to state on this point. However, these results highlight that it is important to take into account the fact that strains in culture can evolve, so that ecophysiological studies should be performed as soon as possible (≤ 1 or 2 years) after *Pseudo-nitzschia* strains have been isolated.

In *P. australis*, the link between growth rate and strain age was probably the outcome of the weak relationship between age and cell size since cell size was sufficient to predict the growth rate. The same relationship was observed for the three species, with a sharp decrease in growth rate below a cell size threshold of 60 µm. Above this size, growth rates were similar in all *P. fraudulenta* strains whatever the cell size. However, above 60 µm in *P. pungens* and *P. australis*, the growth rate also decreased with cell size, although more slowly. Altogether, the growth rate decreased with decreasing cell size. This result is in contradiction with allometric rules generally accepted for phytoplankton populations. These rules predict an increase of growth rates with decreasing cell size due to higher surface-to-volume ratios that, for example, favor higher nutrient uptake (Amato et al. 2005, Von Dassow et al. 2006a, Edwards et al. 2012, Marañón et al. 2013, Otero et al. 2018). Our results therefore show that allometric rules do not apply when dealing with intraspecific diversity in *Pseudo-nitzschia* species. The distinctive feature of the size-growth relationship for our three *Pseudo-nitzschia* species is the sharp decrease of the growth rate in small

cells. Similar results have been reported for *Thalassiosira* species (Chisholm and Costello 1980; Von Dassow et al. 2006). These authors related the decrease of the growth rate in small cells to sexual reproduction. In contrast, in the present study, the lowest growth rates did not coincide with gametangia size ranges, and might rather represent a decrease in metabolism efficiency when cells approached their minimum viable size. Emphasizing this point, we often observed cells studied here displayed abnormal valve shapes in the smallest-size strains (data not shown), suggesting deficient valve deposition as reported by Von Dassow et al. (2006). In natural populations, the fact that small cells may be physiologically less efficient could explain why these size ranges are rarely observed: small cells may not be competitive enough to outcompete larger cells and survive. Consequently, it is important to pay attention to cell size in addition to strain age. Strains of large to medium cell sizes (≥ gametangia sizes) should be used for ecophysiological studies on *Pseudo-nitzschia* species. Furthermore, choosing strains of similar cell sizes appears to be an important prerequisite for comparative (inter- or intraspecific) studies.

As far as domoic acid (cDA and dDA) production is concerned, strain age had no significant influence in the three species. However, a few young *P. pungens* strains presented higher cDA concentrations than the others, whatever their age. Beyond inter-specific differences, this could explain why a decrease in cDA with time in culture was previously reported in the literature (Lelong et al. 2012 and references herein), in contrast with the present results.

As for the influence of cell size, we found the highest dDA concentrations in some large *P. fraudulenta* F1 strains, and the highest cDA concentrations in some large *P. pungens* strains. However, there was no clear evidence of an influence of cell size on *P. fraudulenta* and *P. pungens* DA production since large strains of these two species also exhibited very low cDA and dDA concentrations. These results do not confirm that DA production systematically decreases with decreasing cell size, as reported in *P. multiseries* and *P. multistriata* (Bates et al. 1999, Mafra et al. 2009, Amato et al. 2010). However, they are not completely in disagreement for some strains, stressing once more the high intraspecific variability characteristic of *Pseudo-nitzschia* species. This great variability was also highlighted by the cDA and dDA concentrations measured in the F1 strains, which were not related to concentrations in parental strains. This result is in agreement with Amato et al. (2010), who studied *P. multistriata* and concluded that the inheritance of the ability to produce DA was not a simple Mendelian process.

Our results revealed that cDA concentrations could be predicted from cell size by a Gaussian model in *P. australis*. This is not completely in contradiction with previous results reporting a decrease in cDA with decreasing cell size (Bates et al. 1999, Mafra et al. 2009, Amato et al. 2010). Our cell size range was greater than in any other study because we took into account very large strains issued from initial cells obtained in mating experiments. In the literature, the decrease in cDA corresponds to sizes ranging from medium-sized to small cells (Bates et al. 1999, Mafra et al. 2009, Amato et al. 2010). We also observed a decrease in cDA with decreasing cell size *in P. australis* within that same size range. In addition, we brought supplementary information to currently available data about the relationship showing that showing that medium-sized cells are the most toxic ones and large cells issued from sexual reproduction present cDA concentrations comparable to small cells. These observations show that cDA concentrations are not linearly related to cell size in *P. australis*. Furthermore, the evolution of cDA and dDA concentrations suggests that they are not characteristic of any given strain because DA production is not stable over a whole life time in *P. australis*, in contrast to results reported for *P. multistriata* (Amato et al. 2010). This discrepancy highlights the fact that (i) the relationship between cell size and DA production is species-specific, and (ii) it is important to study the whole size range of a species before drawing conclusions on this relationship.

The striking result of this study is that the increase in cDA in *P. australis* coincided with the size range within which the cells reached the gametangia stage, while dDA also increased in the larger gametangial cells. We can therefore hypothesize that the physiological changes occurring when vegetative cells become sexualized also result in an increase of DA production. During the sexual reproduction process (gametogenesis, fertilization, and auxosporulation), the cells cannot carry out photosynthesis and probably other metabolic pathways any more. Preparing vegetative cells for this step probably includes increasing cell metabolism efficiency and/or modifications of metabolic pathways to increase cellular quotas of/ the required cellular metabolites (Pan et al. 1998). This probable reorientation of the metabolism may also favor DA synthesis pathways. Bates et al. (1999) hypothesized that the ability of cells to produce domoic acid was not related to cell size but to general physiological changes. Our results suggest that these physiological changes can be linked to the life cycle and especially the sexualization of vegetative cells, at least for *P. australis*. Domoic acid synthesis pathways involve the Krebs cycle and the formation of derived compounds, *e.g.* glutamate and geranyl pyrophosphate (Pan et al. 1998, Brunson et al. 2018). We can hypothesize that in *P. australis* the change in metabolism that the cells undergo for their sexualization affects these metabolic pathways, resulting in an increase in DA production.

Therefore, the increase in DA cellular content in gametangia cells might be a "physiological coincidence". However, the role of this toxin still remains to be deciphered, so we can also wonder if DA could play a role in *P. australis* sexual reproduction. In pennate diatoms, interactions between sexualized cells are needed to trigger gametogenesis. The increased production of DA (and especially dissolved DA) therefore raises questions on the potential role of this toxin as a pheromone (previously mentioned by Lelong et al. 2012). Interestingly, the only pheromone identified in a pennate diatom up to now is a cyclic dipeptide derived from proline, whose synthesis is thus linked to amino acid biosynthesis (Guillard et al. 2013, Frenkel et al. 2014). It is however surprising that a similar link between DA production and life cycle was not found in the two other *Pseudo-nitzschia* species which present the same sexual reproduction pattern. In addition, cells may be more vulnerable during sexual reproduction, so domoic acid could act as a grazer deterrent: its production has been shown to increase in the presence of copepods (Harðardóttir et al. 2015, Tammilehto et al. 2015). Finally, different studies also showed an allelopathic effect of *Pseudo-nitzschia* or DA addition on different phytoplankton species (Lundholm et al. 2005, Smeti et al. 2015, Sobrinho et al. 2017, Van Meerssche et al. 2018). Higher DA production may therefore also represent an ecological advantage that could offset the growth arrest/decrease during sexual events in *Pseudo-nitzschia* blooms.

The link between DA and cell size, and therefore DA and life cycle stages, suggests that *P. australis* life cycle probably impacts bloom toxicity. First, *P. australis* populations can be more or less toxic depending on their cell size spectra. Cell size distribution varies across years in natural populations (D'Alelio et al. 2010), this might partly explain inter-annual variations in bloom toxicity. Furthermore, when a sexual event occurs in a natural population, it results in the production of initial cells and thus in a shift in size distribution towards large cells (Holtermann et al. 2010). During a *P. australis* bloom, this process is expected to result in a decrease in DA concentration in the population, especially as the large cells with slightly higher growth rates will progressively outnumber smaller cells in this population (Armbrust and Chisholm 1992). Life cycle events could therefore also impact DA concentrations in natural populations at the scale of a bloom.

CONCLUSION

This study characterizes the toxicity and cell size - life cycle relationship in three *Pseudo-nitzschia* species. Even if we evidenced species-specific characteristics, the importance of intra-specific variability proves that the number of studied strains *per* species greatly influences the

conclusions on *Pseudo-nitzschia* physiology. Furthermore, our results advocate for the use of *Pseudo-nitzschia* strains not more than one or two years after their isolation, and of cell sizes at or above gametangia size when studying cellular metabolism. However, as far as toxicity is concerned, our results do not support the hypothesis of a decrease in DA production with time in culture in these three species. Most importantly, this study shows that *P. australis* cDA can be predicted from cell size by a non-linear relationship. In this species, cDA is maximum in medium-sized cells at the gametangia stage of their life cycle. These results suggest that either the metabolic changes occurring in gametangia cells favor DA production as compared to vegetative cells, or that DA is involved in sexual reproduction. The *Pseudo-nitzschia* life cycle may therefore influence the toxicity of blooms. Furthermore, the cell size – cDA relationship revealed by our results may be useful to predict bloom toxicity based on the cell size spectra of a *P. australis* population. Finally, a comparative understanding of the cellular metabolism of *P. australis* at different life cycle stages may help to identify the DA biosynthesis pathway.

ACKNOWLEDGEMENTS

The authors thank Dr. Didier Goux for his assistance with species identification by TEM, the BOREA laboratory staff for help with the experiments and Annie Buchwalter for English corrections. We are most grateful to Dr. Catherine Dreanno for identification by sequencing of *Pseudo-nitzschia* strains. We thank Dr. Amandine Caruana (Ifremer, Laboratoire Phycotoxines, Nantes, France), Dr. Elisabeth Nézan, and Dr. Nicolas Chomérat (Ifremer, LER/BO, Concarneau, France) for a *P. australis* parental strain. We also thank the two anonymous reviewers for their comments and suggestions that helped improve the manuscript. This work was supported by the PseudoPhy project (2015-2019) funded by Agence de l'eau Seine-Normandie and by an INSU EC2CO (France) grant. Aurore Sauvey received a PhD fellowship from the Ministère de la Recherche et de l'Enseignement Supérieur, and this paper is part of her Ph.D. thesis.

REFERENCES

Ajani, P.A., Verma, A., Lassudrie, M., Doblin, M.A. & Murray, A. 2018. A new diatom species *P . hallegraeffii* sp . nov . belonging to the toxic genus *Pseudo-nitzschia* (Bacillariophyceae) from the East Australian Current. PLoS ONE 13(4):e0195622.

Allen, A.E., Dupont, C.L., Obornik, M., Horak, A., Nunes-Nesi, A., McCrow, J.P., Zheng, H., Johnson, D.A., Hu, H., Fernie, A.R. & Bowler, C. 2011. Evolution and metabolic significance

679 of the urea cycle in photosynthetic diatoms. *Nature*. 473(7346):203.
680 Álvarez, G., Uribe, E., Quijano-Scheggia, S., López-Rivera, A., Mariño, C. & Blanco, J. 2009.
681 Domoic acid production by *Pseudo-nitzschia australis* and *Pseudo-nitzschia calliantha*
682 isolated from North Chile. *Harmful Algae*. 8:938–45.
683 Amato, A., Orsini, L., D'Alelio, D. & Montresor, M. 2005. Life cycle, size reduction patterns, and
684 ultrastructure of the pennate planktonic diatom *Pseudo-nitzschia delicatissima*
685 (Bacillariophyceae). *J. Phycol.* 41:542–56.
686 Amato, A., Kooistra, W.H., Ghiron, J.H.L., Mann, D.G., Pröschold, T. & Montresor, M. 2007.
687 Reproductive isolation among sympatric cryptic species in marine diatoms. *Protist*, 158(2),
688 193-207.
689 Amato, A., Lüdeking, A. & Kooistra, W.H.C.F. 2010. Intracellular domoic acid production in
690 *Pseudo-nitzschia multistriata* isolated from the Gulf of Naples (Tyrrhenian Sea, Italy).
691 *Toxicon*. 55:157–61.
692 Armbrust, E.V. & Chisholm, S.W. 1992. Patterns of cell size change in marine centric diatom:
693 variability evolving from clonal isolates. *J. Phycol.* 28:146–56.
694 Armstrong, R.A., Peterson, M.L., Lee, C. & Wakeham, S.G. 2009. Settling velocity spectra and the
695 ballast ratio hypothesis. *Deep. Res. Part II Top. Stud. Oceanogr*. 56:1470–8.
696 Bailleul, B., Berne, N., Murik, O., Petroutsos, D., Prihoda, J., Tanaka, A., Villanova, V., Bligny, R.,
697 Flori, S., Falconet, D., Krieger-Liszkay, A., Santabarbara, S., Rappaport, F., Joliot, P.,
698 Tirichine, L., Falkowski, P.G., Cardol, P., Bowler, C. & Finazzi, G. 2015. Energetic coupling
699 between plastids and mitochondria drives CO_2 assimilation in diatoms. *Nature*. 524(7565):366.
700 Bargu, S., Powell, C.L., Wang, Z., Doucette, G.J. & Silver, M.W. 2008. Note on the occurrence of
701 *Pseudo-nitzschia australis* and domoic acid in squid from Monterey Bay, CA (USA). *Harmful*
702 *Algae*. 7:45–51.
703 Bates, S., Garrison, D. & Horner, R. 1998. Bloom dynamics and physiology producing *Pseudo-*
704 *nitzschia* species. In: Anderson, D.M., A.D. Cembella, and G.M. Hallegraeff [eds.].
705 Physiological ecology of harmful algal blooms, p. 267-292. Springer-Verlag. Heidelberg. .
706 Bates, S.S., Hiltz, M.F. & Léger, C. 1999. Domoic acid toxicity of large new cells of *Pseudo-*
707 *nitzschia multiseries* resulting from sexual reproduction. *Sixth Can. Work. Harmful Mar.*
708 *Algae*. 21–6.
709 Baugh, K.A., Bush, J.M., Bill, B.D., Lefebvre, K.A. & Trainer, V.L. 2006. Estimates of specific
710 toxicity in several *Pseudo-nitzschia* species from the Washington coast , based on culture and
711 field studies. 28:403–7.
712 Brunson, J.K., Mckinnie, S.M.K., Chekan, J.R., Mccrow, J.P., Miles, Z.D., Bertrand, E.M.,

713 Bielinski, V.A., Luhavaya, H., Obornik, M., Smith, G.J., Hutchins, D.A., Allen, A.E. &
714 Moore, B.S. 2018. Biosynthesis of the neurotoxin domoic acid in a bloom-forming diatom.
715 *Science.* 365:1356–8.
716 Calu, G., Martin-Jezequel, V., Lefau, E., Sechet, V., Lassus, P., Weigel, P., & Amzil, Z. (2009).
717 The influence of nitrogen speciation on growth and toxicity of *Pseudo-nitzschia multiseries*
718 and *P. pungens* in batch and continuous cultures. In *Seventh International Conference on*
719 *Molluscan Shellfish Safety, Éditions Quæ, Nantes* (p. 7).
720 Chepurnov, V.A., Mann, D.G., Sabbe, K., Vannerum, K., Casteleyn, G., Verleyen, E., Peperzak, L.
721 and Vyverman, W. 2005. Sexual reproduction, mating system, chloroplast dynamics and
722 abrupt cell size reduction in *Pseudo-nitzschia pungens* from the North Sea (Bacillariophyta).
723 *Eur. J. Phycol.* 40:379–95.
724 Chepurnov, V.A., Mann, D.G., Sabbe, K. & Vyverman, W. 2004. Experimental studies on sexual
725 reproduction in Diatoms. *International Review of Cytology: A Survey of Cell Biology* 237
726 (2004): 91-154.
727 Chisholm, S.W. & Costello, J.C. 1980. Influence of environmental factors and population
728 composition on the timing of cell division in *Thalassiosira fluviatilis* (Bacillariophyceae)
729 grown on light/dark cycles. *Journal of Phycology.* 16: 375-383.
730 Cusack, C., Raine, R. & Patching, J.W. 2004. Occurrence of species from the genus P*seudo-*
731 *nitzschia* peragallo in Irish waters. *Biol. Environ.* 104:55–74.
732 Cusack, C.K., Bates, S.S., Quilliam, M.A., Patching, J.W. & Raine, R. 2002. Confirmation of
733 domoic acid production by *Pseudo-nitzschia australis* (Bacillariophyceae) isolated from Irish
734 waters. *Journal of Phycology.* 28: 604-607.
735 D'Alelio, D., Amato, A., Luedeking, A. & Montresor, M. 2009. Sexual and vegetative phases in the
736 planktonic diatom *Pseudo-nitzschia multistriata*. *Harmful Algae.* 8:225–32.
737 D'Alelio, D., D'Alcalà, M.R., Dubroca, L., Sarno, D., Zingone, A. & Montresor, M. 2010. The time
738 for sex: A biennial life cycle in a marine planktonic diatom. *Limnol. Oceanogr.* 55:106–14.
739 Davidovich, N.A. 1994. Factors controlling the size of initial cells in diatoms. *Russ. J. Plant*
740 *Physiol.* 41:220–4.
741 Davidovich, N.A., Kaczmarska, I. & Ehrman, J.M. 2010. Heterothallic and homothallic sexual
742 reproduction in *Tabularia fasciculata* (Bacillariophyta). *Fottea*. 10:251–66.
743 Davidovich, N. A., Gastineau, R., Gaudin, P., Davidovich, O.I. & Mouget, J.L. 2012. Sexual
744 reproduction in the newly-described blue diatom, *Haslea karadagensis*. *Fottea*. 12:219–29.
745 Davidovich, N. a & Bates, S.S. 1998. Sexual reproduction in the pennate diatoms *Pseudo-nitzschia*
746 *multiseries* and *P. pseudodelicatissima* (Bacillariophyceae). *J. Phycol.* 34:126–37.

747 Edlund, M.B. & Bixby, R.J. 2001. Intra- and inter-specific differences in gametangial and initial
748 cell size in diatoms. *Proceedings of the 16th international diatom symposium*. Vol. 25. Athens:
749 Faculty of Biology, University of Athens, 2001.
750 Edlund, M.B. & Stoermer, E.F. 1997. Ecological, evolutionary, and systematic significance of
751 diatom life histories. *J. Phycol.* 33:897–918.
752 Edwards, K.F., Thomas, M.K., Klausmeier, C.A. & Litchman, E. 2012. Allometric scaling and
753 taxonomic variation in nutrient utilization traits and maximum growth rate of phytoplankton.
754 *Limnol. Oceanogr.* 57:554–66.
755 Fehling, J., Davidson, K., Bolch, C.J. & Bates, S.S. 2004. Growth and domoic acid production by
756 *Pseudo-nitzschia seriata* (Bacillariophyceae) under phosphate and silicate limitation. *J.*
757 *Phycol.* 40:674–83.
758 Fernandes, L.F., Hubbard, K. A., Richlen, M.L., Smith, J., Bates, S.S., Ehrman, J., Léger, C., Mafra
759 Jr. L.L., Kulis, D., Quilliam, M., Libera, K., McCauley, L. and Anderson, D.M. 2014.
760 Diversity and toxicity of the diatom *Pseudo-nitzschia* Peragallo in the Gulf of Maine,
761 Northwestern Atlantic Ocean. *Deep. Res. Part II Top. Stud. Oceanogr.* 103:139–62.
762 Frenkel, J., Vyverman, W. & Pohnert, G. 2014. Pheromone signaling during sexual reproduction in
763 algae. *Plant J.* 79:632–44.
764 Frøsig Gai, F., Kirketerp Hedemand, C., Louw, D.C. & Grobler, K. 2018. Morphological ,
765 molecular and toxigenic characteristics of Namibian *Pseudo- nitzschia* species – including
766 *Pseudo-nitzschia bucculenta* sp . nov . *Harmful Algae*. 76:80–95.
767 Fuchs, N., Scalco, E., Kooistra, W.H.C.F., Assmy, P. & Montresor, M. 2013. Genetic
768 characterization and life cycle of the diatom *Fragilariopsis kerguelensis*. *Eur. J. Phycol.*
769 48:411–26.
770 Fuchs, N., Scalco, E., Kooistra, W.H.C.F., Assmy, P. & Montresor, M. 2013. Genetic
771 characterization and life cycle of the diatom *Fragilariopsis kerguelensis*. *Eur. J. Phycol.*
772 48:411–26.
773 Garrison, D., Conrad, S., Eilers, P. & Waldrom, E. 1992. Confirmation of domoic acid production
774 by *Pseudo-nitzschia australis* (Bacillariophyceae) cultures. *J. Phycol.* 28:604–7.
775 Godhe, A. & Rynearson, T. 2017. The role of intraspecific variation in the ecological and
776 evolutionary success of diatoms in changing environments. *Philosophical Transactions of the*
777 *Royal Society B: Biological Sciences.* 372.1728: 20160399.
778 Guillard, J., Frenkel, J., Devos, V., Sabbe, K., Paul, C., Rempt, M., Inzé, D., Pohnert, G.,
779 Vuylsteke, M., and Vyverman, W. 2013. Metabolomics enables the structure elucidation of a
780 diatom sex pheromone. *Angew. Chemis Int. Ed.* 52:854–7.

781 Hamm, C.E., Merkel, R., Springer, O., Jurkojc, P., Maier, C., Prechtel, K. & Smetacek, V. 2003.
782 Architecture and material properties of diatom shells provide effective mechanical protection.
783 *Nature*, 421(6925), 841.
784 Harðardóttir, S., Pančić, M., Tammilehto, A., Krock, B., Møller, E., Nielsen, T. & Lundholm, N.
785 2015. Dangerous relations in the Arctic marine food web: Interactions between toxin
786 producing *Pseudo-nitzschia* diatoms and *Calanus* Copepodites. *Mar. Drugs*. 13:3809–35.
787 Hasle, G.R. 2002. Are most of the domoic acid-producing species of the diatom genus *Pseudo-*
788 *nitzschia* cosmopolites? *Harmful Algae*. 1:137–46.
789 Hense, I. & Beckmann, A. 2015. A theoretical investigation of the diatom cell size reduction-
790 restitution cycle. *Ecol. Modell.* 317:66–82.
791 Hiltz, M., Bates, S.S. & Kaczmarska, I. 2000. Effect of light: dark cycles and cell apical length on
792 the sexual reproduction of the pennate diatom *Pseudo-nitzschia multiseries*
793 (Bacillariophyceae) in culture. *Phycologia*. 39:59–66.
794 Holtermann, K.E., Bates, S.S., Trainer, V.L., Odell, A. & Armbrust, E.V. 2010. Mass sexual
795 reproduction in the toxigenic diatoms *Pseudo-nitzschia australis* and *P. pungens*
796 (Bacillariophyceae) on the Washington coast, USA. *J. Phycol.* 46:41–52.
797 Howard, M.D.A., Cochlan, W.P., Ladizinsky, N. & Kudela, R.M. 2007. Nitrogenous preference of
798 toxigenic *Pseudo-nitzschia australis* (Bacillariophyceae) from field and laboratory
799 experiments. *Harmful Algae*. 6:206–17.
800 Jewson, D.H. 1992. Size reduction, reproductive strategy and the life cycle of a centric diatom. Phil.
801 Trans. R. Soc. Lond. B 336.1277: 191-213.
802 Kaczmarska, I., Poulíčková, A., Sato, S., Edlund, M.B., Idei, M., Watanabe, T. & Mann, D.G. 2013.
803 Proposals for a terminology for diatom sexual reproduction, auxospores and resting stages.
804 *Diatom Res.* 1–32.
805 Keller, M.D., Selvin, R.C., Claus, W. & Guillard, R.R.. 1987. Media for the culture of oceanic
806 ultraphytoplankton. *J. Phycol.* 23:633–8.
807 Klein, C., Claquin, P., Bouchart, V., Le Roy, B. & Véron, B. 2010. Dynamics of *Pseudo-nitzschia*
808 spp. and domoic acid production in a macrotidal ecosystem of the Eastern English Channel
809 (Normandy, France). *Harmful Algae*. 9:218–26.
810 Lakeman, M.B., von Dassow, P. & Cattolico, R.A. 2009. The strain concept in phytoplankton
811 ecology. *Harmful Algae*. 8:746–58.
812 Lelong, A., Hégaret, H., Soudant, P. & Bates, S.S. 2012. *Pseudo-nitzschia* (Bacillariophyceae)
813 species, domoic acid and amnesic shellfish poisoning : revisiting previous paradigms.
814 *Phycologia*. 51:168–216.

Lema, K.A., Latimier, M., Nézan, É., Fauchot, J. & Le Gac, M. 2017. Inter- and intra-specific growth and domoic acid production in relation to nutrient ratios and concentrations in *Pseudo-nitzschia*: phosphate an important factor. *Harmful Algae*. 64:11–9.

Lewis, W.M. 1984. The diatom sex clock and its evolutionary significance. *The American Naturalist* 123.1: 73-80.

Lewis, W.M. 1987. The cost of sex. In: Stearns S.C. (eds). *The evolution of sex and its consequences*. Experientia Supplementum, vol. 55, Birkhäuser, Basel, 33-57.

Li, Y., Huang, C.X., Xu, G.S., Lundholm, N., Teng, S.T., Wu, H. & Tan, Z. 2017. *Pseudo-nitzschia simulans* sp. nov. (Bacillariophyceae), the first domoic acid producer from Chinese waters. *Harmful Algae*. 67:119–30.

Lim, H.C., Lim, P.T., Teng, S.T., Bates, S.S. & Leaw, C.P. 2014. Genetic structure of *Pseudo-nitzschia pungens* (Bacillariophyceae) populations: Implications of a global diversification of the diatom. *Harmful Algae*. 37:142–52.

Lim, H.C., Teng, S.T., Leaw, C.P. & Lim, P.T. 2013. Three novel species in the *Pseudo-nitzschia pseudodelicatissima* complex: *P. batesiana* sp. nov., *P. lundholmiae* sp. nov., and *P. fukuyoi* sp. nov. (Bacillariophyceae) from the Strait of Malacca, Malaysia. *J. Phycol.* 49:902–16.

Liu, H., Kelly, M.S., Campbell, D. a, Dong, S.L., Zhu, J.X. & Wang, S.F. 2007. Exposure to domoic acid affects larval development of king scallop *Pecten maximus* (Linnaeus, 1758). *Aquat. Toxicol.* 81:152–8.

Lundholm, N., Daugbjerg, N. & Moestrup, Ø. 2002. Phylogeny of the Bacillariaceae with emphasis on the genus *Pseudo-nitzschia* (Bacillariophyceae) based on partial LSU rDNA. *Eur. J. Phycol.* 37:115–34.

Lundholm, N., Hansen, P.J. & Kotaki, Y. 2005. Lack of allelopathic effects of the domoic acid-producing marine diatom *Pseudo-nitzschia multiseries*. *Mar. Ecol. Prog. Ser.* 288:21–33.

Mafra, L.L., Bricelj, V.M., Ouellette, C., Léger, C. & Bates, S.S. 2009. Mechanisms contributing to low domoic acid uptake by oysters feeding on *Pseudo-nitzschia* cells. I. Filtration and pseudofeces production. *Aquat. Biol.* 6:201–12.

Maldonado, M.T., Hughes, M.P., Rue, E.L. & Wells, M.L. 2002. The effect of Fe and Cu on growth and domoic acid production by *Pseudo-nitzschia multiseries* and *Pseudo-nitzschia australis*. *Limnol. Oceanogr.* 47:515–26.

Mann, D.G. 1999. The species concept in diatoms. *Phycologia*. 38:437–95.

Mann, D.G., Chepurnov, V.A. & Idei, M. 2003. Mating system, sexual reproduction, and auxosporulation in the anomalous raphid diatom *Eunotia* (Bacillariophyta)1. *J. Phycol.* 39:1067–84.

849 Mann, D.G. & Vanormelingen, P. 2013. An inordinate fondness? the number, distributions, and
850 origins of diatom species. *J. Eukaryot. Microbiol.* 60:414–20.
851 Marañón, E., Cermeño, P., López-Sandoval, D.C., Rodríguez-Ramos, T., Sobrino, C., Huete-
852 Ortega, M., Blanco, J.M. & Rodriguez, J. 2013. Unimodal size scaling of phytoplankton
853 growth and the size dependence of nutrient uptake and use. *Ecol. Lett.* 16:371–9.
854 Martin-Jézéquel, V., Calu, G., Candela, L., Amzil, Z., Jauffrais, T., Séchet, V. & Weigel, P. 2015.
855 Effects of organic and inorganic nitrogen on the growth and production of domoic acid by
856 *Pseudo-nitzschia multiseries* and *P. australis* (bacillariophyceae) in culture. *Mar. Drugs*.
857 13:7067–86.
858 Not, F., Siano, R., Kooistra, W.H.C.F., Simon, N., Vaulot, D. & Probert, I. 2012. Diversity and
859 ecology of eukaryotic marine phytoplankton. *Advances in Botanical Research*. Vol. 64.
860 Academic Press, 2012. 1-53.
861 Orive, E., Pérez-Aicua, L., David, H., García-Etxebarria, K., Laza-Martínez, A., Seoane, S. &
862 Miguel, I. 2013. The genus *Pseudo-nitzschia* (Bacillariophyceae) in a temperate estuary with
863 description of two new species: *Pseudo-nitzschia plurisecta* sp. nov. and *Pseudo-nitzschia*
864 *abrensis* sp. nov. *J. Phycol.* 49:1192–206.
865 Otero, J., Bode, A., Álvarez-salgado, X.A. & Varela, M. 2018. Role of functional trait variability in
866 the response of individual phytoplankton species to changing environmental conditions in a
867 coastal upwelling zone. 596:33–47.
868 Pan, Y., Bates, S.S. & Cembella, A.D. 1998. Environmental stress and domoic acid production by
869 *Pseudo-nitzschia*: a physiological perspective. *Nat. Toxins*. 6:127–35.
870 Pan, Y., Subba Rao, D., Mann, K.H., Rg, B. & Pocklington, R. 1996a. Effects of silicate limitation
871 on production of domoic acid , a neurotoxin , by the diatom *Pseudo-nitzschia multiseries*. I.
872 Batch culture studies. *Marine ecology progress series* 131 (1996): 225-233.
873 Pan, Y., Subba Rao, D. V & Mann, K.H. 1996b. Changes in domoic acid production and cellular
874 chemical composition of the toxigenic diatom *Pseudo-nitzschia multiseries* under phosphate
875 limitation. *Marine ecology progress series* 131 (1996): 235-243.
876 Quijano-Scheggia, S., Garcés, E., Andree, K.B., De la Iglesia, P., Diogène, J., Fortuño, J.M. &
877 Camp, J. 2010. *Pseudo-nitzschia* species on the Catalan coast: characterization and
878 contribution to the current knowledge of the distribution of this genus in the Mediterranean
879 Sea. *Sci. Mar.* 74:395–410.
880 Radan, R.L. & Cochlan, W.P. 2018. Differential toxin response of *Pseudo-nitzschia multiseries* as a
881 function of nitrogen speciation in batch and continuous cultures, and during a natural
882 assemblage experiment. *Harmful Algae*. 73:12–29.

Rhodes, L., Jiang, W., Knight, B., Adamson, J., Smith, K., Langi, V. & Edgar, M. 2013. The genus *Pseudo-nitzschia* (Bacillariophyceae) in New Zealand: Analysis of the last decade's monitoring data. *New Zeal. J. Mar. Freshw. Res.* 47:490–503.Santiago-Morales, I.S. & García-Mendoza, E. 2011. Growth and domoic acid content of *Pseudo-nitzschia australis* isolated from northwestern Baja California, Mexico, cultured under batch conditions at different temperatures and two Si:NO_3 ratios. *Harmful Algae*. 12:82–94.

Sato, S., Beakes, G., Idei, M., Nagumo, T. & Mann, D.G. 2011. Novel sex cells and evidence for sex pheromones in diatoms. *PLoS One*. 6: e26923.

Schwarz, R., Wolf, M. & Müller, T. 2009. A probabilistic model of cell size reduction in *Pseudo-nitzschia delicatissima* (Bacillariophyta). *J. Theor. Biol.* 258:316–22.

Smeti, E., Roelke, D.L., Gremion, G., Linhart, J.M., Danielidis, D.B. & Spatharis, S. 2015. Potential mechanisms of coexistence between two globally important *Pseudo-nitzschia* (Bacillariophyta) species. *Hydrobiologia*. 762:89–101.

Sobrinho, B.F., De Camargo, L.M., Sandrini-Neto, L., Kleemann, C.R., Da Costa Machado, E. & Mafra, L.L. 2017. Growth, toxin production and allelopathic effects of *Pseudo-Nitzschia multiseries* under Iron-enriched conditions. *Marine drugs* 15: 331.

Tammilehto, A., Nielsen, T.G., Krock, B., Møller, E.F. & Lundholm, N. 2015. Induction of domoic acid production in the toxic diatom *Pseudo-nitzschia seriata* by calanoid copepods. *Aquat. Toxicol.* 159:52–61.

Teng, S.T., Lim, H.C., Lim, P.T., Dao, V.H., Bates, S.S. & Leaw, C.P. 2014. *Pseudo-nitzschia kodamae* sp. nov. (Bacillariophyceae), a toxigenic species from the Strait of Malacca, Malaysia. *Harmful Algae*. 34:17–28.

Teng, S.T., Tan, S.N., Lim, H.C., Dao, V.H., Bates, S.S. & Leaw, C.P. 2016. High diversity of *Pseudo-nitzschia* along the northern coast of Sarawak (Malaysian Borneo), with descriptions of *P. bipertita* sp. nov. and *P. limii* sp. nov. (Bacillariophyceae)1. *Journal of phycology* 52: 973-989.

Thessen, A. E., Bowers, H. a. & Stoecker, D.K. 2009. Intra- and interspecies differences in growth and toxicity of *Pseudo-nitzschia* while using different nitrogen sources. *Harmful Algae*. 8:792–810.

Thorel, M., Fauchot, J., Morelle, J., Raimbault, V., Le Roy, B., Miossec, C., Kientz-Bouchart, V. & Claquin, P. 2014. Interactive effects of irradiance and temperature on growth and domoic acid production of the toxic diatom *Pseudo-nitzschia australis* (Bacillariophyceae). *Harmful Algae*. 39:232–41.

Thorel, M., Claquin, P., Schapira, M., Le Gendre, R., Riou, P., Goux, D., Le Roy, B., Raimbault,

V., Deton-Cabanillas, A.-F., Bazin, P., Kientz-Bouchart, V. & Fauchot, J. 2017. Nutrient ratios influence variability in *Pseudo-nitzschia* species diversity and particulate domoic acid production in the Bay of Seine (France). *Harmful Algae*. 68:192–205.

Trainer, V.L., Bates, S.S., Lundholm, N., Thessen, A.E., Cochlan, W.P., Adams, N.G. & Trick, C.G. 2012. *Pseudo-nitzschia* physiological ecology, phylogeny, toxicity, monitoring and impacts on ecosystem health. *Harmful Algae*. 14:271–300.

Van Meerssche, E., Greenfield, D.I. & Pinckney, J.L. 2018. Coastal eutrophication and freshening: Impacts on *Pseudo-nitzschia* abundance and domoic acid allelopathy. *Estuar. Coast. Shelf Sci.* 209:70–9.

Vanormelingen, P., Vanelslander, B., Sato, S., Gillard, J., Trobajo, R., Sabbe, K. & Vyverman, W. 2013. Heterothallic sexual reproduction in the model diatom *Cylindrotheca*. *Eur. J. Phycol.* 48:93–105.

Villac, M.C., Roelke, D.L., Chavez, F.P., Cifuentes, L.A. & Fryxell, G.A. 1993. *Pseudo-nitzschia australis* Frenguelli and related species from the west coast of the U.S.A.: occurrence and domoic acid production. *J. Shellfish Res.* 12:457–65.

Von Dassow, P., Chepurnov, V.A. & Armbrust, E.V. 2006a. Relationships between growth rate, cell size, and induction of spermatogenesis in the centric diatom *Thalassiosira weissflogii* (Bacillariophyta). *J. Phycol.* 42:887–99.

Table 1. Strains of *P. australis*, *P. pungens*, and *P. fraudulenta* used for mating and batch culture experiments. (A) for strains isolated from the Atlantic and (EC) for strains isolated from the English Channel. The age of the strain (in months, calculated from the date of isolation) and the cell size length (cell size) are indicated for each experiment.

Species	Strain information			Age of strain (month)	Cell size length (µm)
	Collection reference	Origin (Sampling zone or crossing)	Isolation date		
P. australis	IFR-PAU-010	Ouessant (A)	07/2015	5	50
	PNaus P1D2	Camaret-sur-Mer (A)	03/2014	21	44
	PNaus P3B2	Plouzané (A)	03/2014	21	49
	PNaus 02T	Arcachon Bay (A)	04/2016	9 - 12 - 14 - 16	69 - 63 - 60 - 57
	PNaus P6B3	Plouzané (A)	04/2014	20 - 26	42 - 35
	PNaus F1-1A	P6B3 x P2B1			83
	PNaus F1-4A	P6B3 x P6C1			73
	PNaus F1-5	P6B3 x P1A3			97 - 82 - 65 - 61 - 57
	PNaus F2-1B	F1-5 x F1-1A			127 - 106
P. pungens	PNpun 47	Cabourg (EC)	08/2011	59	48
	PNpun 66	Ouistreham (EC)	09/2011	51 - 58	41 - 47
	PNpun 79	Cabourg (EC)	05/2012	50	52
	PNpun 88	Cabourg (EC)	07/2012	48	47
	PNpun 89	Cabourg (EC)	07/2012	41 - 48	42 - 49
	PNpun 129	Luc-sur-mer (EC)	07/2016	2	75
	PNpun 130	Luc-sur-mer (EC)	07/2016	2	95
	PNpun 133	Luc-sur-mer (EC)	07/2016	3	109
	PNpun 134	Luc-sur-mer (EC)	07/2016	3	102
	PNpun 136	Saint-Vaast-la-Hougue (EC)	07/2016	3	85
	PNpun F1-7A	66 x 89			157 - 175
	PNpun F1-7B	66 x 89			153
	PNpun F1-11	66 x 47			153
P. fraudulenta	PNfra 1	Cabourg (EC)	08/2011	62	27
	PNfra 10	Cabourg (EC)	08/2011	51 - 59	45 - 39
	PNfra 30	Cabourg (EC)	10/2011	49 - 57	41 - 36
	PNfra 31	COMOR 41 (EC)	07/2011	64	31
	PNfra 126	Luc-sur-mer (EC)	11/2015	3	65
	PNfra 132	Luc-sur-mer (EC)	10/2015	3	68
	PNfra 162	Saint-Vaast-la-Hougue (EC)	05/2016	5	69
	PNfra F1-8D	30 x 31			107 - 87
	PNfra F1-9A	10 x 31			78
	PNfra F1-9B	10 x 31			113 - 92
	PNfra F1-14A	10 x 1			110
	PNfra F1-14B	10 x 1			113

FIGURES LEGENDS

Figure 1. Mean size of initial cells as a function of mean size of parent strains in *P. australis*, *P. pungens*, and *P. fraudulenta*. Standard deviations represent the minimum and maximum sizes measured for initial cells and represent the variance for parental cells.

Figure 2. Size range of vegetative cells (white) and gametangia (grey and hatched pattern) in *P. australis*, *P. pungens*, and *P. fraudulenta*. Crosses and dots correspond to cell sizes for which mating experiments were performed. Crosses: no sexual reproduction observed. Hatched pattern and white dots: incomplete sexual reproduction observed (without initial cell production). Light grey and dark grey dots: complete sexual reproduction observed (with initial cell production). The size percentage was calculated based on the maximal initial size. 85 mating experiments were made to define the gametangia size range for *P. australis*, 40 for *P. pungens*, and 89 for *P. fraudulenta*. 193 cells were measured to determine the vegetative cell size range for *P. australis*, 334 cells for *P. pungens*, and 551 cells for *P. fraudulenta*.

Figure 3. (A) Growth rate (µ, day^{-1}) as a function of the age of the strains (months) since their isolation from natural populations in *P. australis* (n = 9), *P. pungens* (n = 12), and *P. fraudulenta* (n = 9) (F1 strains from sexual reproduction are not present in this graph). (B) Growth rate (µ, day^{-1}) as a function of the cell size (µm) for all strains studied in *P. australis* (n = 18), *P. pungens* (n = 16), and *P. fraudulenta* (n = 16).

Figure 4. Cellular domoic acid content (cDA, $fg.cell^{-1}$) as a function of cell size (µm): (A) in *P. australis* and (B) in *P. pungens* and *P. fraudulenta*. Data come from the cDA measurements made in the batch experiments on the second day of the stationary phase linked to a phosphate or silicate limitation.

Figure 5. Dissolved domoic acid (dDA, $fg.cell^{-1}$) as a function of cell size (µm): (A) in *P. australis* and (B) in *P. pungens* and *P. fraudulenta*. Data come from the dDA measurements made in the batch experiments on the second day of the stationary phase linked to a phosphate or silicate limitation.

Figure 6. Monitoring of the cellular domoic acid content (cDA, $fg.cell^{-1}$) of four strains of *P. australis* during their decrease in cell size.

SUPPLEMENTARY FIGURES LEGENDS

Figure S1. Optical microscopy observation of *Pseudo-nitzschia australis* strain (PNaus P6B3) with abnormal valve shapes in small cells.

Figure S2. Relationship between cell size and strain age (month) since their isolation from the natural environment in *P. australis* (n = 9), *P. pungens* (n = 12), and *P. fraudulenta* (n = 9) (F1 strains are not taken into account). Linear regressions are not significant ($P > 0.05$).

Figure S3. Cellular domoic acid content (cDA, $fg.cell^{-1}$, mean ± SD) under phosphate limitation (black bars) or silicate limitation (grey bars) in *P. australis* (n = 18), *P. pungens* (n = 16), and *P. fraudulenta* (n = 16). The letters a, b and c indicate the significant differences ($P < 0.001$).

Figure S4. Cellular domoic acid content (cDA, $fg.cell^{-1}$) as a function of the age of the strain (months) since their isolation from natural populations: (A) in *P. australis* (n = 9) and (B) in *P. pungens* (n = 12) and *P. fraudulenta* (n = 9).

Figure S5. Dissolved domoic acid (dDA, $fg.cell^{-1}$) as a function of the age of the strain (months) since their isolation from natural populations: (A) *P. australis* (n = 9) and (B) in *P. pungens* (n = 12) and *P. fraudulenta* (n = 9).

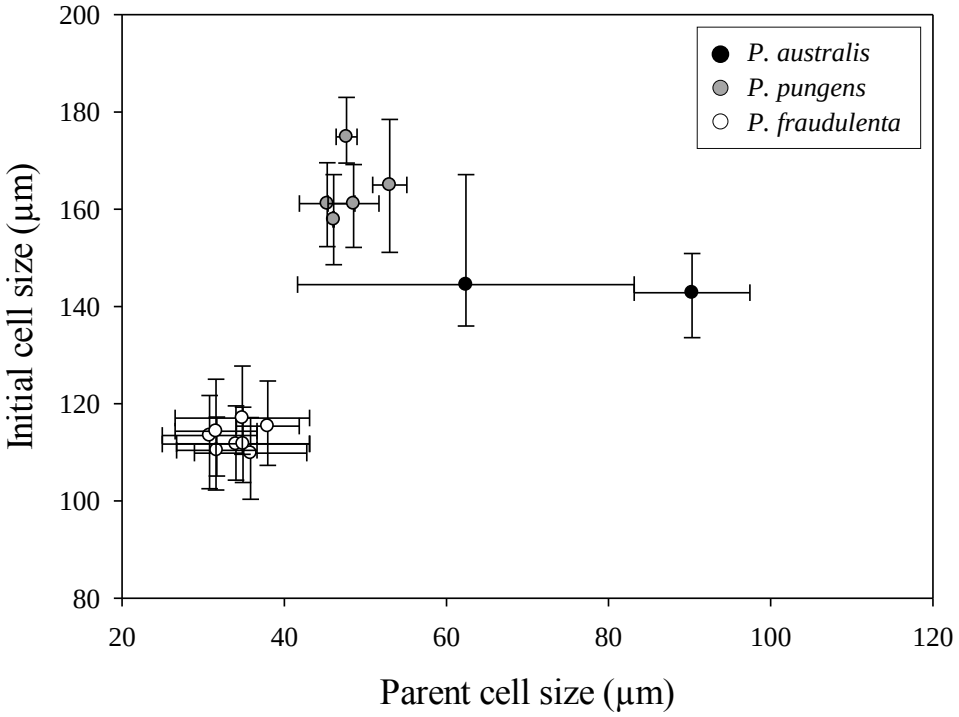
200
180
160
140
120
100
80
Initial cell size (µm)
20
40
60
80
100
120
Parent cell size (µm)
P. australis
P. pungens
P. fraudulenta

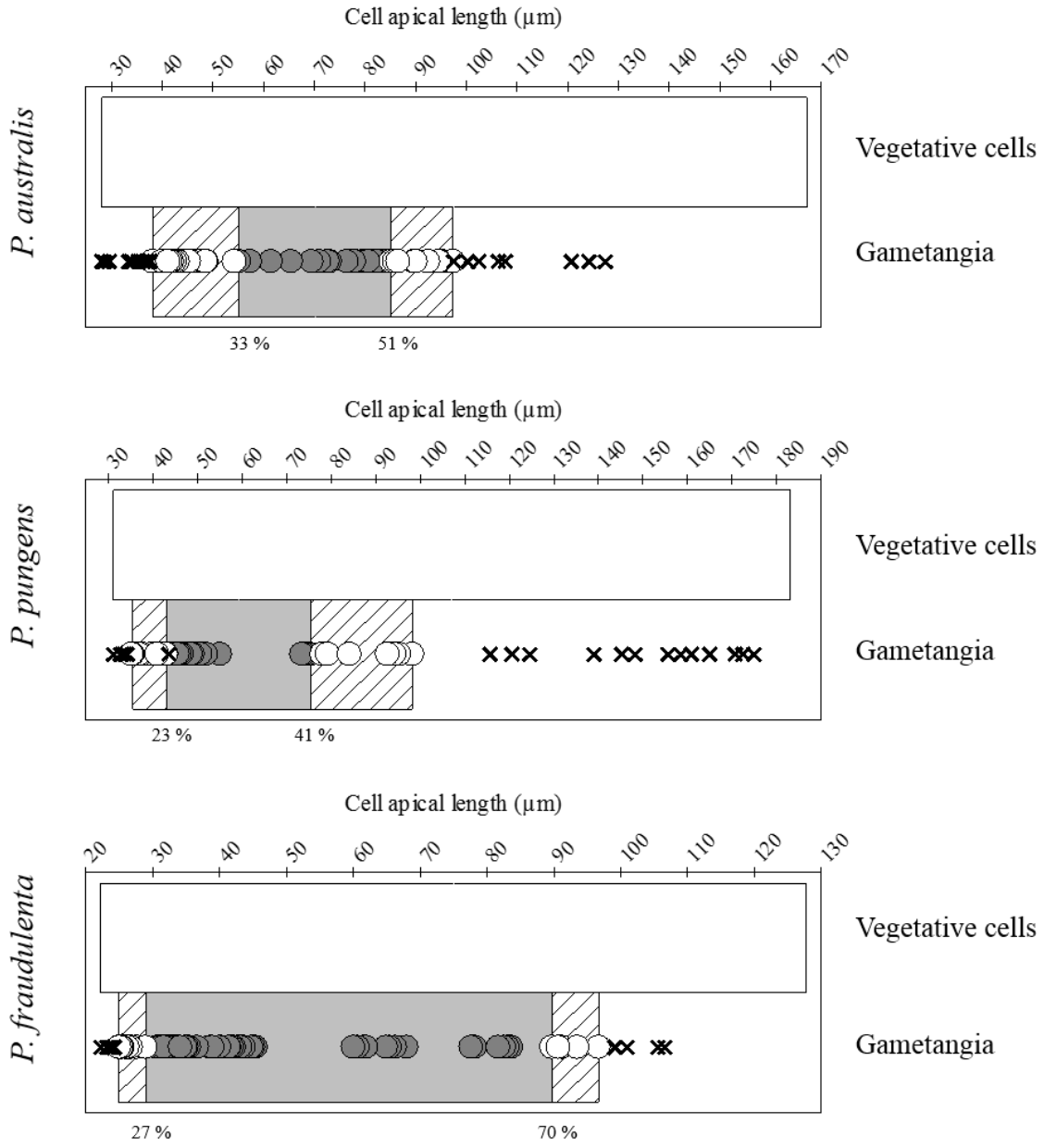
Cell apical length (µm)
30 40 50 60 70 80 90 100 110 120 130 140 150 160 170
P. australis
Vegetative cells
Gametangia
33 %
51 %
Cell apical length (µm)
30 40 50 60 70 80 90 100 110 120 130 140 150 160 170 180 190
P. pungens
Vegetative cells
Gametangia
23 %
41 %
Cell apical length (µm)
20 30 40 50 60 70 80 90 100 110 120 130
P. fraudulenta
Vegetative cells
Gametangia
27 %
70 %

Figure 2

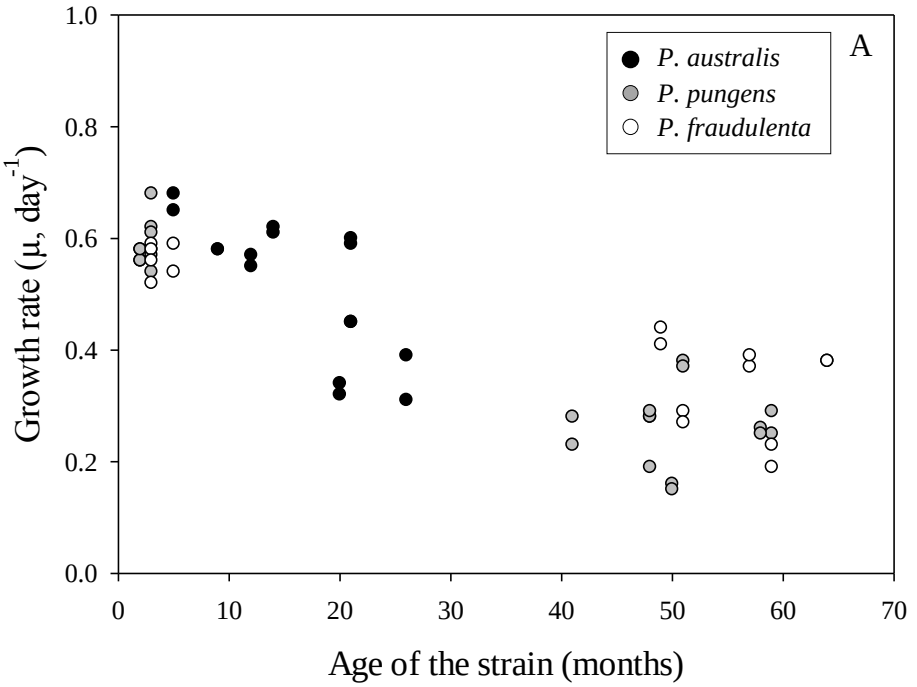
A
P. australis
P. pungens
P. fraudulenta
Growth rate (μ, day-1)
Age of the strain (months)
0.0
0.2
0.4
0.6
0.8
1.0
0
10
20
30
40
50
60
70

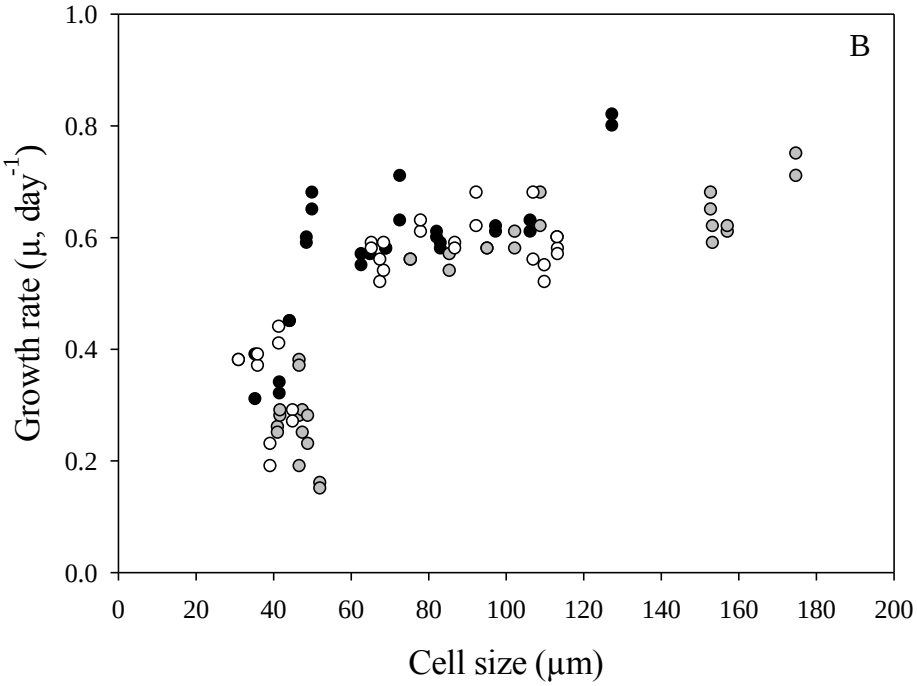
B
Growth rate (μ, day-1)
Cell size (μm)
0.0
0.2
0.4
0.6
0.8
1.0
0
20
40
60
80
100
120
140
160
180
200

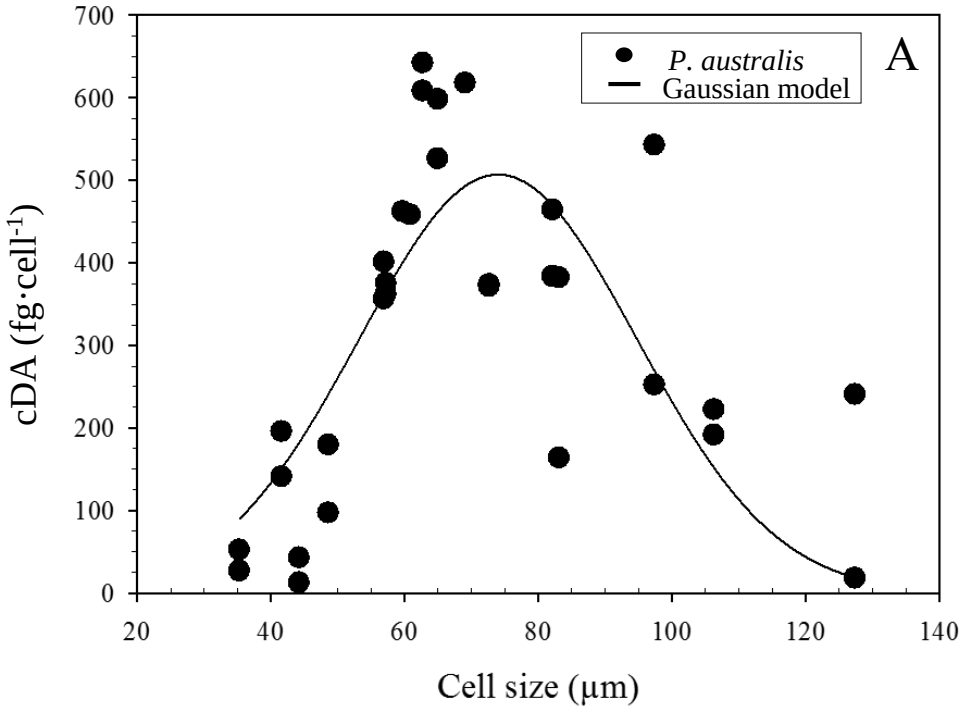
A
P. australis
Gaussian model
cDA (fg·cell-1)
Cell size (µm)
0
100
200
300
400
500
600
700
20
40
60
80
100
120
140

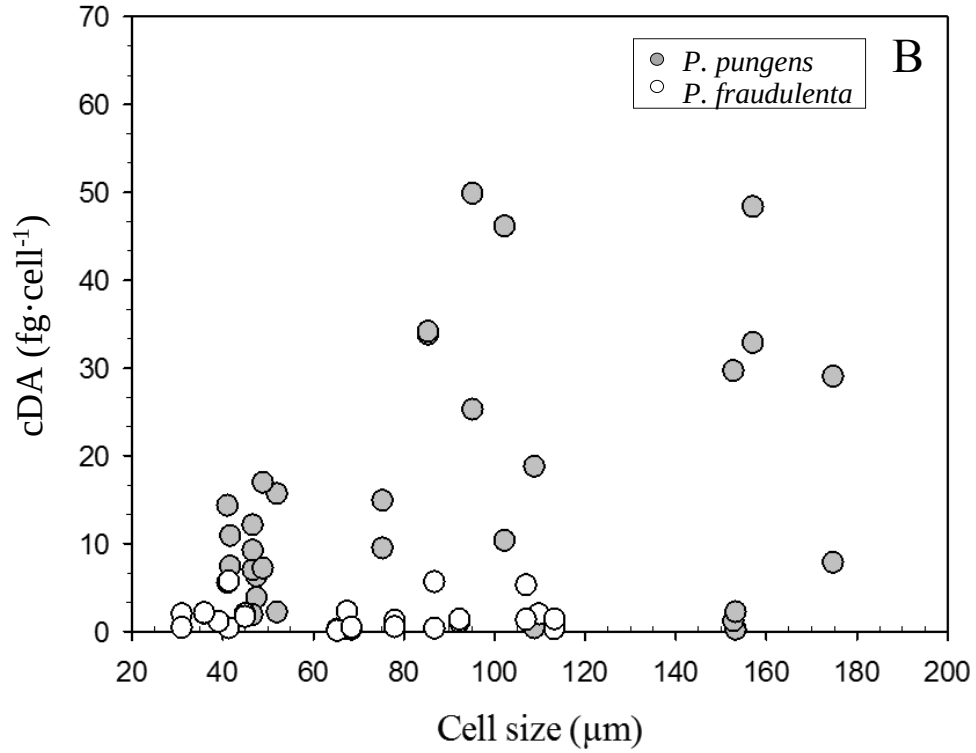
B
P. pungens
P. fraudulenta
cDA (fg·cell-1)
Cell size (µm)
0
10
20
30
40
50
60
70
20
40
60
80
100
120
140
160
180
200

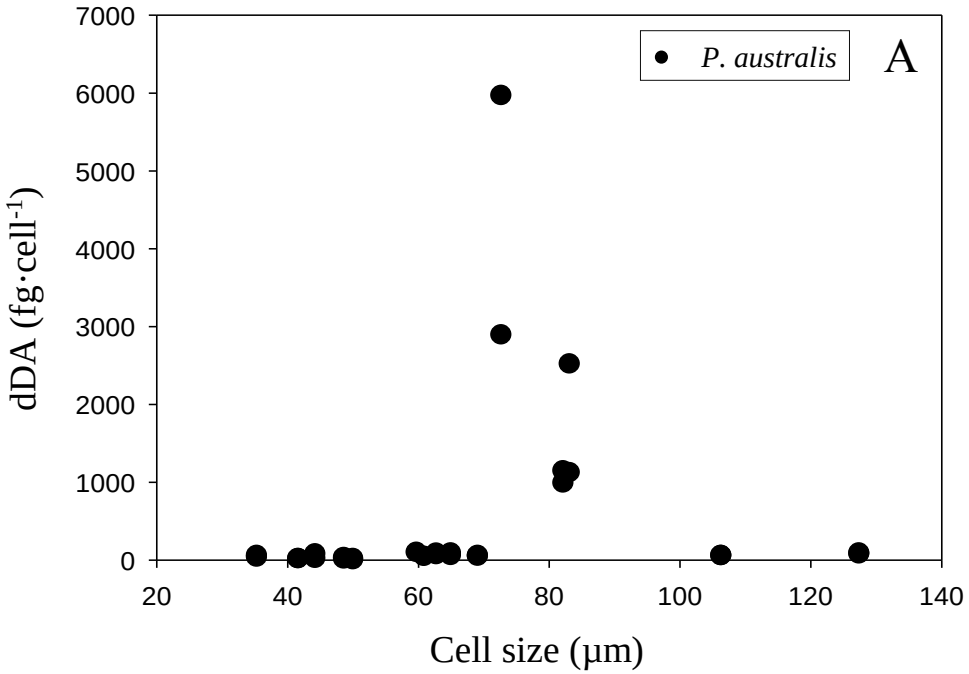
7000
6000
5000
4000
3000
2000
1000
0
dDA (fg·cell-1)
20
40
60
80
100
120
140
Cell size (µm)
P. australis
A

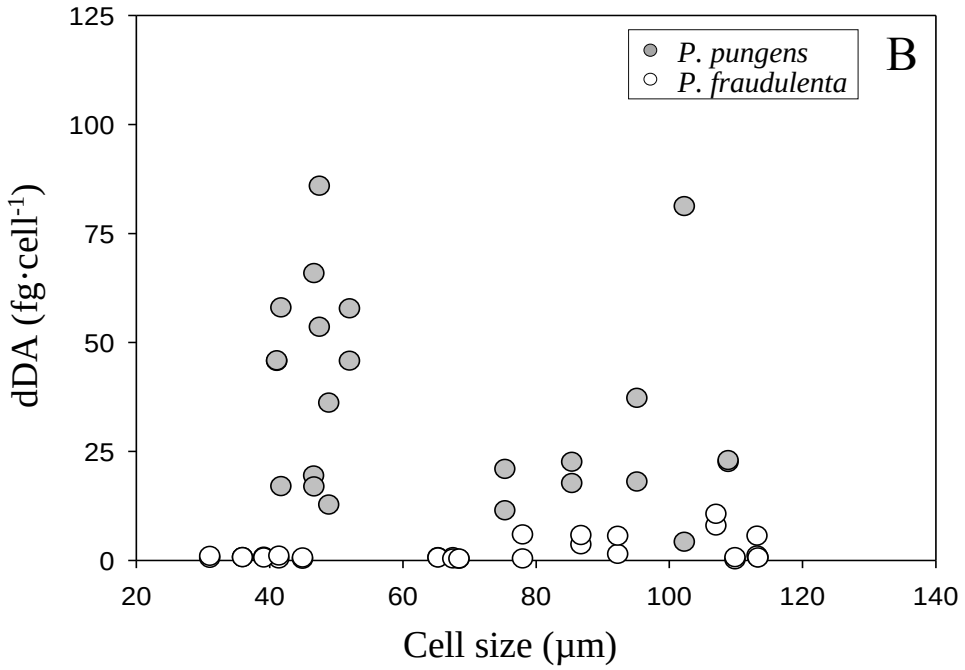
125
100
75
50
25
0
dDA (fg·cell-1)
20
40
60
80
100
120
140
Cell size (µm)
P. pungens
P. fraudulenta
B

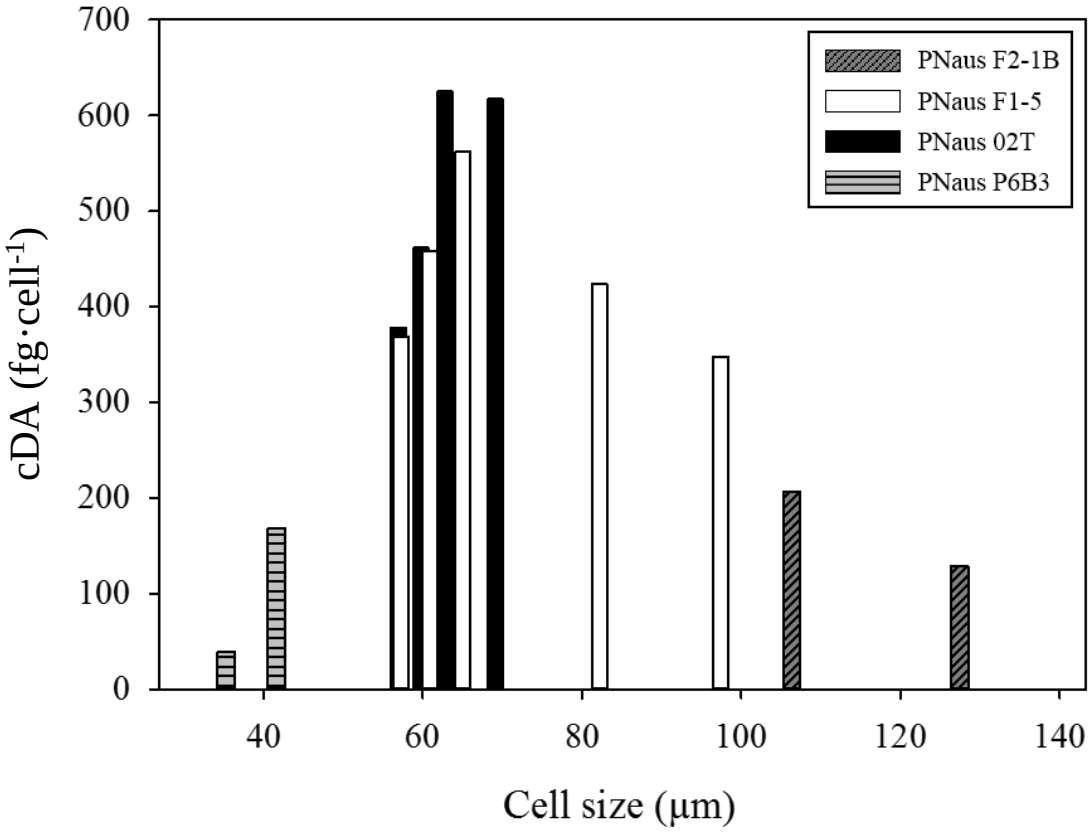
700
600
500
400
300
200
100
0
cDA (fg·cell-1)
40
60
80
100
120
140
Cell size (µm)
PNaus F2-1B
PNaus F1-5
PNaus 02T
PNaus P6B3

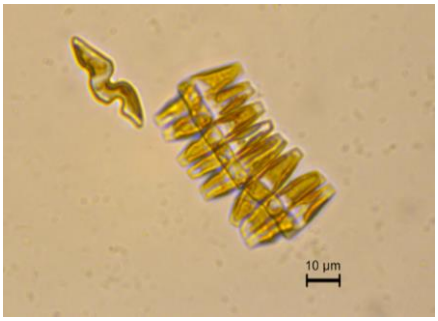
10 µm

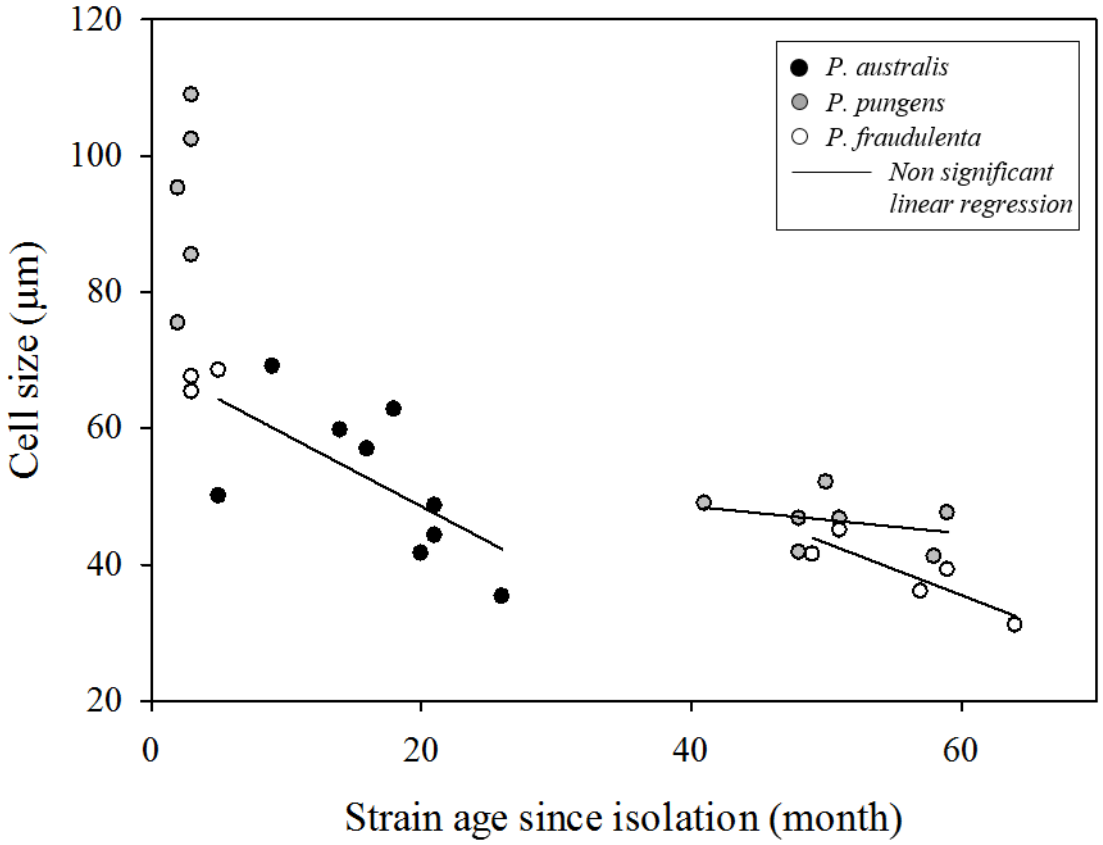

Figure S1. Relationship between cell size and strain age (month) since their isolation from the natural environment in *P. australis*, *P. pungens* and *P. fraudulenta* (F1 strains are not taken into account). Linear regressions are not significant ($P > 0.05$).

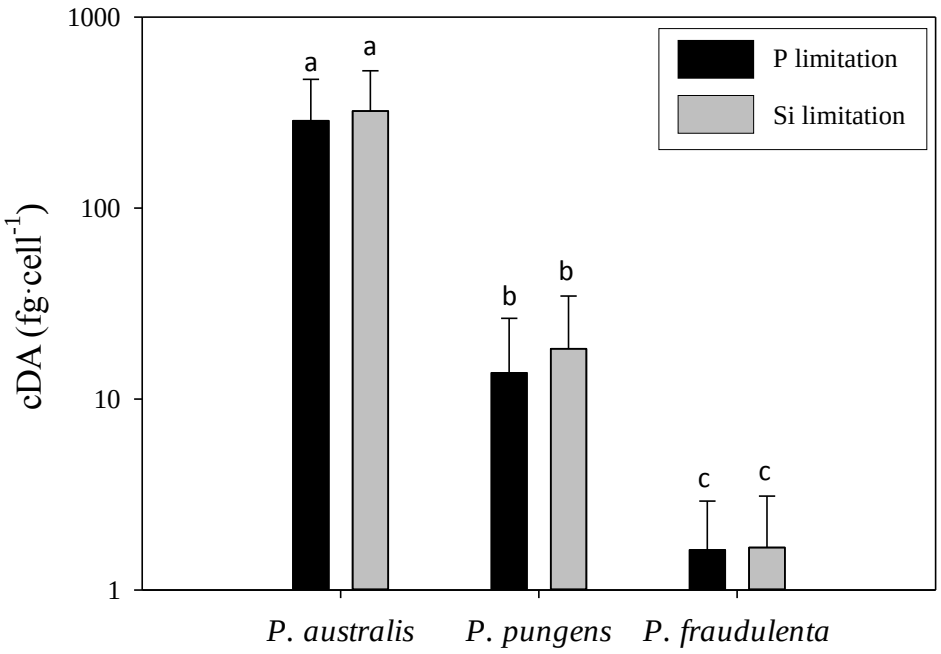

Figure S3. Cellular domoic acid content (cDA, fg.cell^{-1}, mean ± SD) under phosphate limitation (black bars) or silicate limitation (grey bars) in *P. australis* (n = 18), *P. pungens* (n = 16), and *P. fraudulenta* (n = 16). The letters a, b and c indicate the significant differences ($P < 0.001$).

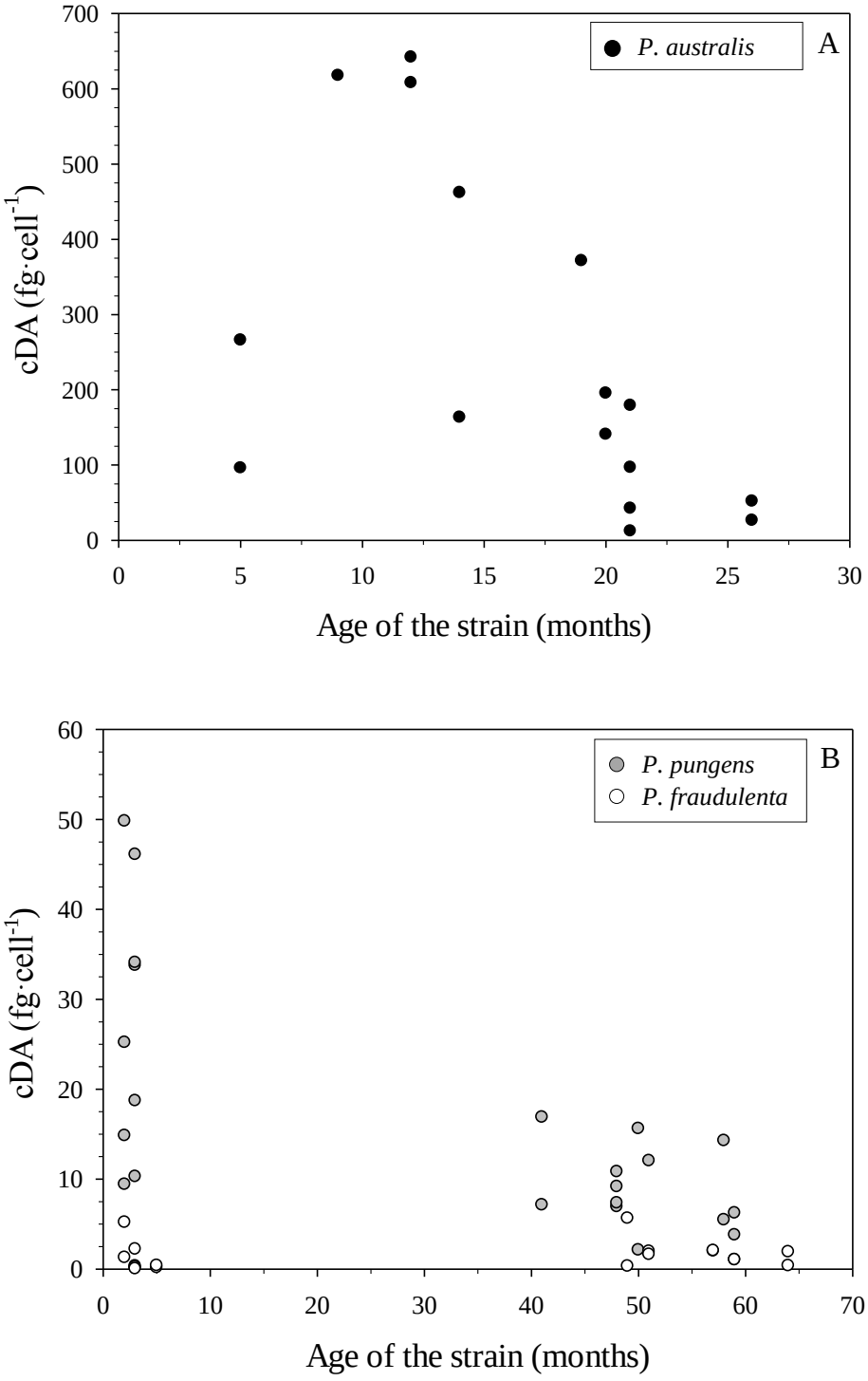

Figure S4. Cellular domoic acid content (cDA, fg.cell^{-1}) as a function of the age of the strain (months) since their isolation from natural populations: (A) in *P. australis* (n = 9) and (B) in *P. pungens* (n = 12) and *P. fraudulenta* (n = 9).

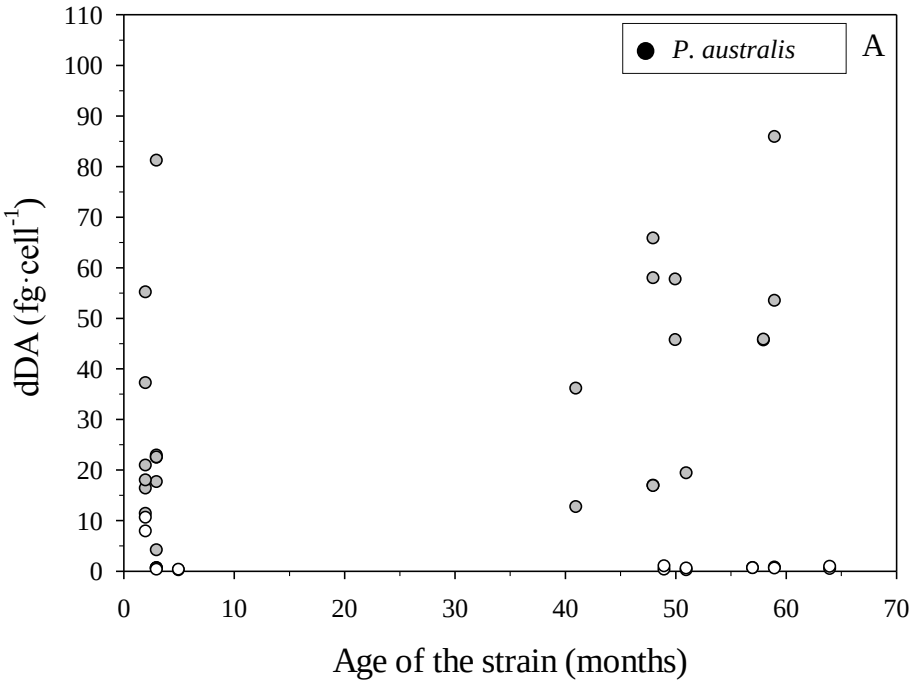

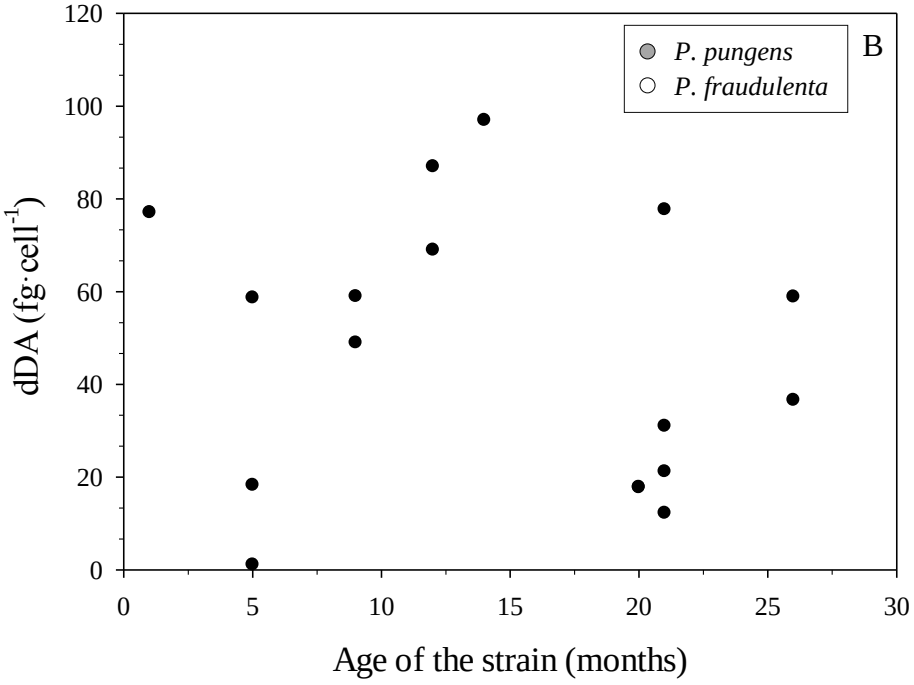

Figure S5. Dissolved domoic acid (dDA, fg.cell^{-1}) as a function of the age of the strain (months) since their isolation from natural populations: (A) *P. australis* (n = 9) and (B) in *P. pungens* (n = 12) and *P. fraudulenta* (n = 9).

FIGURES LEGENDS

Figure 1. Mean size of initial cells as a function of mean size of parent strains in *P. australis*, *P. pungens*, and *P. fraudulenta*. Standard deviations represent the minimum and maximum sizes measured for initial cells and represent the variance for parental cells.

Figure 2. Size range of vegetative cells (white) and gametangia (grey and hatched pattern) in *P. australis*, *P. pungens*, and *P. fraudulenta*. Crosses and dots correspond to cell sizes for which mating experiments were performed. Crosses: no sexual reproduction observed. Hatched pattern and white dots: incomplete sexual reproduction observed (without initial cell production). Light grey and dark grey dots: complete sexual reproduction observed (with initial cell production). The size percentage was calculated based on the maximal initial size. 85 mating experiments were made to define the gametangia size range for *P. australis*, 40 for *P. pungens*, and 89 for *P. fraudulenta*. 193 cells were measured to determine the vegetative cell size range for *P. australis*, 334 cells for *P. pungens*, and 551 cells for *P. fraudulenta*.

Figure 3. (A) Growth rate (µ, day^{-1}) as a function of the age of the strains (months) since their isolation from natural populations in *P. australis* (n = 9), *P. pungens* (n = 12), and *P. fraudulenta* (n = 9) (F1 strains from sexual reproduction are not present in this graph). (B) Growth rate (µ, day^{-1}) as a function of the cell size (µm) for all strains studied in *P. australis* (n = 18), *P. pungens* (n = 16), and *P. fraudulenta* (n = 16).

Figure 4. Cellular domoic acid content (cDA, $fg.cell^{-1}$) as a function of cell size (µm): (A) in *P. australis* and (B) in *P. pungens* and *P. fraudulenta*. Data come from the cDA measurements made in the batch experiments on the second day of the stationary phase linked to a phosphate or silicate limitation.

Figure 5. Dissolved domoic acid (dDA, $fg.cell^{-1}$) as a function of cell size (µm): (A) in *P. australis* and (B) in *P. pungens* and *P. fraudulenta*. Data come from the dDA measurements made in the batch experiments on the second day of the stationary phase linked to a phosphate or silicate limitation.

Figure 6. Monitoring of the cellular domoic acid content (cDA, $fg.cell^{-1}$) of four strains of *P. australis* during their decrease in cell size.

SUPPLEMENTARY FIGURES LEGENDS

Figure S1. Optical microscopy observation of *Pseudo-nitzschia australis* strain (PNaus P6B3) with abnormal valve shapes in small cells.

Figure S2. Relationship between cell size and strain age (month) since their isolation from the natural environment in *P. australis* (n = 9), *P. pungens* (n = 12), and *P. fraudulenta* (n = 9) (F1 strains are not taken into account). Linear regressions are not significant ($P > 0.05$).

Figure S3. Cellular domoic acid content (cDA, $fg.cell^{-1}$, mean ± SD) under phosphate limitation (black bars) or silicate limitation (grey bars) in *P. australis* (n = 18), *P. pungens* (n = 16), and *P. fraudulenta* (n = 16). The letters a, b and c indicate the significant differences ($P < 0.001$).

Figure S4. Cellular domoic acid content (cDA, $fg.cell^{-1}$) as a function of the age of the strain (months) since their isolation from natural populations: (A) in *P. australis* (n = 9) and (B) in *P. pungens* (n = 12) and *P. fraudulenta* (n = 9).

Figure S5. Dissolved domoic acid (dDA, $fg.cell^{-1}$) as a function of the age of the strain (months) since their isolation from natural populations: (A) *P. australis* (n = 9) and (B) in *P. pungens* (n = 12) and *P. fraudulenta* (n = 9).

Species	Strain information			Age of strain (month)	Cell apical length (µm)
	Collection reference	Origin (Sampling zone or crossing)	Isolation date		
P. australis	IFR-PAU-010	Ouessant (A)	07/2015	5	50
	PNaus P1D2	Camaret-sur-Mer (A)	03/2014	21	44
	PNaus P3B2	Plouzané (A)	03/2014	21	49
	IFR-PAU-16.2	Arcachon Bay (A)	05/2016	9 - 12 - 14 - 16	69 - 63 - 60 - 57
	PNaus P6B3	Plouzané (A)	04/2014	20 - 26	42 - 35
	PNaus F1-1A	P6B3 x P2B1			83
	PNaus F1-4A	P6B3 x P6C1			73
	PNaus F1-5	P6B3 x P1A3			97 - 82 - 65 - 61 - 57
	PNaus F2-1B	F1-5 x F1-1A			127 - 106
P. pungens	PNpun 47	Cabourg (EC)	08/2011	59	48
	PNpun 66	Ouistreham (EC)	09/2011	51 - 58	41 - 47
	PNpun 79	Cabourg (EC)	05/2012	50	52
	PNpun 88	Cabourg (EC)	07/2012	48	47
	PNpun 89	Cabourg (EC)	07/2012	41 - 48	42 - 49
	PNpun 129	Luc-sur-mer (EC)	07/2016	2	75
	PNpun 130	Luc-sur-mer (EC)	07/2016	2	95
	PNpun 133	Luc-sur-mer (EC)	07/2016	3	109
	PNpun 134	Luc-sur-mer (EC)	07/2016	3	102
	PNpun 136	Saint-Vaast-la-Hougue (EC)	07/2016	3	85
	PNpun F1-7A	66 x 89			157 - 175
	PNpun F1-7B	66 x 89			153
	PNpun F1-11	66 x 47			153
P. fraudulenta	PNfra 1	Cabourg (EC)	08/2011	62	27
	PNfra 10	Cabourg (EC)	08/2011	51 - 59	45 - 39
	PNfra 30	Cabourg (EC)	10/2011	49 - 57	41 - 36
	PNfra 31	COMOR 41 (EC)	07/2011	64	31
	PNfra 126	Luc-sur-mer (EC)	11/2015	3	65
	PNfra 132	Luc-sur-mer (EC)	10/2015	3	68
	PNfra 162	Saint-Vaast-la-Hougue (EC)	05/2016	5	69
	PNfra F1-8D	30 x 31			107 - 87
	PNfra F1-9A	10 x 31			78
	PNfra F1-9B	10 x 31			113 - 92
	PNfra F1-14A	10 x 1			110
	PNfra F1-14B	10 x 1			113